

# Using Rapid Compression Machines for Chemical Kinetics Studies

Chih-Jen Sung\*

Department of Mechanical Engineering, University of Connecticut, Storrs, CT 06269, USA

Henry J. Curran

Combustion Chemistry Centre, National University of Ireland, Galway, Ireland

## Abstract

Rapid compression machines (RCMs) are used to simulate a single compression stroke of an internal combustion engine without some of the complicated swirl bowl geometry, cycle-to-cycle variation, residual gas, and other complications associated with engine operating conditions. RCMs are primarily used to measure ignition delay times as a function of temperature, pressure, and fuel/oxygen/diluent ratio; further they can be equipped with diagnostics to determine the temperature and flow fields inside the reaction chamber and to measure the concentrations of reactant, intermediate, and product species produced during combustion.

This paper first discusses the operational principles and design features of RCMs, including the use of creviced pistons, which is an important feature in order to suppress the boundary layer, preventing it from becoming entrained into the reaction chamber via a roll-up vortex. The paper then discusses methods by which experiments performed in RCMs are interpreted and simulated. Furthermore, differences in measured ignition delays from RCMs and shock tube facilities are discussed, with the apparent initial gross disagreement being explained by facility effects in both types of experiments. Finally, future directions for using RCMs in chemical kinetics studies are also discussed.

---

\* Corresponding Author: [cjsung@engr.uconn.edu](mailto:cjsung@engr.uconn.edu).

## Contents

1. Introduction .....	3
2. Operational Principles and Design Features of RCMs .....	4
2.1. General Considerations .....	4
2.2. Effect of Fluid Mechanics and Temperature Homogeneity inside an RCM .....	7
3. Interpretation of RCM Data .....	13
3.1. Facility Effect and Heat Loss Characterization .....	13
3.2. Effect of Compression Stroke .....	16
3.3. Comparison of Shock Tube and RCM Data .....	19
3.4. Adequacy of Zero-Dimensional Approach in RCM Modeling .....	21
4. Uncertainties and Issues for RCM Experiments .....	23
5. Diagnostics in RCM Experiments .....	26
6. Concluding Remarks and Future Directions .....	29
Acknowledgements .....	31
References .....	32

## 1. Introduction

Rapid Compression Machines (RCMs) are considered an important experimental device for understanding low-to-intermediate temperature autoignition chemistry under idealized engine-like conditions. RCMs are able to interrogate the region responsible for many of the fuel-specific effects during low-temperature combustion in engines, including combustion phenomena such as two-stage ignition and the negative temperature coefficient (NTC) region of the ignition response. Although shock tubes are ideal for generating a homogenous high pressure and elevated temperature environment downstream of a reflected shock wave, the uniform conditions typically persist for less than 10 ms. Recent efforts, as discussed in the shock tube paper by Hanson and Davidson [1] in this special issue, have modified the driver section to extend shock tube use for longer ignition delays of 50 ms and longer. Nevertheless, RCMs still hold the advantage in terms of capabilities that replicate reasonably well the low-temperature, high-pressure, and high fuel loading combustion conditions of reciprocating engines and gas turbines. In an RCM, experimental durations are longer than typically available in shock tubes. Therefore, an RCM gives accessibility to study autoignition chemistry at elevated pressure under conditions for which reactivity may be too slow for shock tubes. This typically involves temperatures in the range of 600–1100 K. The complementary combination of RCM and shock tube data has allowed the validation and refinement of various reaction mechanisms over a wide range of pressures and temperatures.

Like other experimental facilities, RCMs also have associated challenges. This paper first introduces the principle of RCM operation and then reviews the strengths and limitations of RCM facilities and results, with special emphasis on those aspects related to chemical kinetic model development and validation. In addition, major sources of errors, quantification of uncertainties, and issues for RCM experiments as well as representative RCM results and their complementary relation with shock tubes will be discussed. Note that this paper presents a succinct and informative review focusing on chemical kinetics studies using RCMs under homogeneous conditions. An extensive review of RCM history and applications based on the outcome of the First International RCM Workshop [2] held at Argonne National Laboratory in August 2012 is currently in preparation by a group of workshop participants and will become available in the near future.

The history of compression machines for combustion studies can roughly be classified into three generations. First-generation compression machines were developed by Falk [3] and Dixon *et al.* [4,5] in which the fuel/oxidizer mixtures were continuously compressed using a piston driven by a falling weight or similar mechanism. The compression ratio in these first-generation machines was limited by the force required to oppose the reactor pressure to prevent piston rebound. The primary data obtained from the first-generation machines were ignition temperatures, while information about ignition delay was not available. After realizing the usefulness of ignition delays, second-generation compression machines were developed in which the reactor piston is held in a final position to create a constant volume reaction chamber. Cassel [6], Tizard and co-authors [7–9], Aubert [10], and Fenning and Cotton [11] thus developed compression machines capable of measuring ignition delay times. The first- and second-generation compression machines were limited primarily by the achievable compression ratio and long compression times, leading to the development of the third generation of compression machines. Very fast compression and higher compression ratios were the key features of the third generation compression machines, and thus they were referred to as Rapid Compression

Machines. In the late 1960's Affleck and Thomas [12] developed a rapid compression machine using compressed-gas driven piston assemblies. This permitted studies at higher compression ratios with associated shorter compression times of about 20 ms. Others RCMs developed by Carlier *et al.* [13], Griffiths *et al.* [14], Park at MIT [15], and by Mittal and Sung [16] used similar designs. In addition, a free-piston rapid compression facility was commissioned at the University of Michigan [17]. The high driving forces necessitate mechanisms to halt the piston at the end of stroke. These mechanisms will be discussed in Section 2.1.

## 2. Operational Principles and Design Features of RCMs

### 2.1. General Considerations

An RCM simulates a single compression stroke of an engine, and is simple and relatively easy to operate. The fuel-oxidizer mixture introduced into the reaction chamber is rapidly compressed by a piston assembly in a process relatively close to adiabatic compression. The reactor piston is brought to rest and fixed in place at the end of compression. This rapid compression results in elevated-temperature, high-pressure conditions in the reaction chamber, which can be used to investigate the autoignition characteristics (ignition delay time, heat release rate, etc.) of a given reactive mixture.

In an RCM experiment, the primary data consists of the pressure trace measured in the reaction chamber as a function of time during and after the compression. Typical pressure traces using non-reactive nitrogen and argon as test gases are shown in Fig. 1, demonstrating a rapid rise in pressure during the compression stroke followed by a gradual decrease in pressure due to heat loss from the constant volume reaction chamber at the end of compression. An overlap of four experiments for each test gas is shown in Fig. 1, where time zero is taken as the end of the compression stroke, when the pressure peaks. The operating conditions for the experiments are also indicated in Fig. 1.

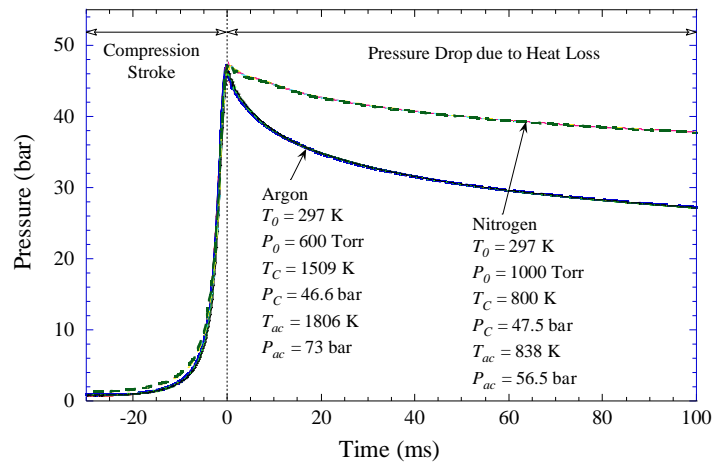


Fig. 1 – Typical pressure traces for inert gas tests, demonstrating experimental repeatability. Subscripts:  $0$  - initial condition;  $C$  - condition at the end of compression;  $ac$  – condition at the end of compression for a truly adiabatic compression. Truly adiabatic compression is calculated using the volumetric compression ratio; see Eq. 1.

Several important features related to RCM performance can be illustrated from these inert gas tests. It is seen in Fig. 1 that the overlapping pressure traces follow each other closely, indicating that highly repeatable experimental conditions are obtained, which is an important feature of RCM design. The RCM experiments depicted in Fig. 1, show that approximately 46% of the pressure rise occurs in the last 2 ms of the compression stroke. Such a rapid pressure rise is desirable in order to minimize the extent of chemical reaction during compression when using a reactive fuel mixture. However, the resulting pressure profile during the compression stroke strongly depends on the RCM's geometry, the machine design, and the operating condition. The data presented in Fig. 1 is taken from [16], which has a relatively fast (20 ms) actuation. Many others have slower rates of pressure rise near the end of compression, especially if piston deceleration is not optimized. For instance, some machines have compression times closer to 50–60 ms, where this can affect chemical induction processes. The issue of slow piston seating at the end of compression or mechanical vibration should also be considered in this context.

In order to avoid significant heat loss and to prevent extensive reactivity before reaching the end of compression, the piston is required to travel very fast. To achieve these high velocities, the piston is usually driven pneumatically. Furthermore, separation of the driving and compression pistons in some RCM designs allows the operation of the machine with a reduced driver gas pressure (compared to reaction chamber pressure) because sufficiently large thrust can still be achieved by using a driving piston of larger diameter in comparison to that of the reactor piston. Instead of a single piston assembly, some RCMs adopt a dual-opposed-piston configuration, originally proposed by Affleck and Thomas [12], in which the twin pistons are simultaneously triggered for the compression event to reduce the compression time and provide a high degree of mechanical balance. Furthermore, minimizing dead volume in the reaction chamber is important in order to ensure a well-defined compression ratio and to ensure that the distribution of charge in the chamber is as close to uniform as possible.

In addition, the pressure traces depicted in Fig. 1 are raw experimental data without any post-processing and are seen to be smooth without significant disturbances. Minimizing the vibrations caused by the abrupt stopping of the piston assembly is another essential feature of an RCM design so that it can yield reliable pressure data. At the end of the compression stroke, the fast-moving piston must stop nearly instantaneously and be locked in the final position. Overshoot and rebound of the piston at the time of stopping have to be avoided in order to ensure a constant volume reaction chamber. Since the stopping of the piston can generate large inertial forces, which in turn can induce vibrations in the machine and deteriorate the quality of the acquired data, a robust and reliable stopping mechanism is required. The effect of vibrations or changes in the volume of the reaction chamber on the acquired data is most severe at the end of compression because of the small clearance used to achieve high compression ratios. Furthermore, uncontrolled inertial forces may lead to mechanical damage and safety concerns.

Various mechanisms have been used to stop the reactor piston at the end of the compression stroke. In early machines, these consisted of using powerful springs, air-cushion systems, plastic deformation of metal, or transferring piston momentum to an auxiliary floating mass to absorb piston energy. However, these methods either require a considerable amount of mechanical manipulation between RCM runs or offer inferior performance. An hydraulic stopping mechanism, first used by Rogowski [18], was demonstrated to overcome these disadvantages. In this hydraulic mechanism, the reactor piston is decelerated and stopped by controlled venting of hydraulic fluid. Various other RCMs, including those currently in operation, have been

successfully developed using this concept. For instance, in [16], the reactor piston is driven pneumatically and decelerated hydraulically using a stopping ring and a groove mechanism. The stopping ring has four steps on it, which progressively reduce the clearance for oil venting as the piston slows down. In the final stage, the piston is held by the force of the driving air, which remains greater than the force of the compressed mixture in the reaction chamber. Based on this design, it was found [16] that during the compression period, the piston initially accelerates at a constant rate. Subsequently, the acceleration decreases and the piston reaches a peak speed. This peak piston speed is maintained until the piston is brought to a stop by a uniform deceleration at the end of compression. Since the piston decelerates at a constant rate, the impact velocity at the end of compression is not large. Alternative stopping mechanism designs also included using the shape of a cam to stop the piston [19] and the interference fit of a polymeric piston in the bore of the reaction chamber in a free-piston rapid compression facility [17].

Furthermore, Fig. 1 indicates that compression is much closer to a truly isentropic compression for nitrogen gas, in that the pressure at the end of compression ( $P_C$ ) is closer to the adiabatic compression pressure ( $P_{ac}$ ) and the reduction in post-compression pressure is more severe for the argon case. This experimental observation is because heat loss is higher when using argon due to the very high compressed gas temperature and its high thermal diffusivity.

Since direct measurement of temperature in an RCM is challenging, the temperature at the end of compression ( $T_C$ ), indicated in Fig. 1, is determined indirectly using the experimental pressure trace. In deducing  $T_C$ , an hypothesis called the “adiabatic core hypothesis” is commonly used [20]. It is assumed that the effect of heat loss to the wall during the compression stroke is limited to a thin boundary layer along the wall of the reaction chamber and the majority of the reaction chamber away from the wall remains unaffected by heat loss. The unaffected region of the chamber is called the core region, in which uniformity of the temperature field is assumed to exist. This means that although compression is not truly adiabatic, the core region of the reaction chamber away from the wall is assumed to be compressed isentropically. If the compression process were truly isentropic, the temperature and pressure at the end of compression would be given by the following relation:

$$\int_{T_0}^{T_{ac}} \frac{1}{\gamma-1} \frac{dT}{T} = \ln(\text{CR}), \quad (1)$$

where  $T_{ac}$  is the temperature at the end of compression for truly adiabatic and reversible compression, CR is the volumetric (geometric) compression ratio,  $T_0$  is the initial temperature before compression begins, and  $\gamma$  is the time-varying, temperature-dependent specific heat ratio. However, due to heat transfer from the hot gases to the wall, the compression is not truly isentropic. Although the actual pressure and temperature are lower than those achieved for isentropic compression, various studies [e.g., 21,22] have shown that it is reasonable to assume an isentropically-compressed core region of the gas mixture, with the effective compression ratio being modified by heat transfer to the wall. Based on the adiabatic core hypothesis, the temperature at the end of compression,  $T_C$ , is determined by using the actual pressure at the end of compression,  $P_C$ , which is measured using a pressure transducer. Therefore, according to the hypothesis,  $T_C$  is calculated according to:

$$\int_{T_0}^{T_C} \frac{\gamma}{\gamma-1} \frac{dT}{T} = \ln\left(\frac{P_C}{P_0}\right), \quad (2)$$

where  $P_0$  is the initial pressure and the other variables are the same as in Eq. 1. The difference between the calculated  $T_C$  and  $T_{ac}$  also indicates the degree to which the compression deviates

from the truly isentropic process. Furthermore, as shown in the above equation, the compression ratio as well as the initial pressure, temperature, and composition of the mixture can be varied to control the pressure and temperature histories in RCM runs.

For a reactive mixture, when suitable conditions of pressure and temperature exist, ignition is observed after a certain ignition delay time, as shown in Figs. 2(a) and 2(b) for single-stage and two-stage ignition phenomena, respectively. Ignition delay times, such as first-stage and total (first- and second-stage), are usually defined as the time from the end of the compression stroke, when the peak in pressure during compression is observed, to the time of the rapid rise in pressure due to the respective ignition responses. Thus, an RCM gives a direct measure of the ignition delay time. However, it must be noted that the induction period does not proceed at a constant temperature, as discussed in Section 3.1. Figures 2(a) and 2(b) also demonstrate the repeatability of experiments under the same conditions, as all of the pressure traces closely follow each other. Moreover, both the first- and second-stage ignition delay times match very well for all of the repeated experiments, as shown in Fig. 2(b). The steep rise in the pressure at the end of the second-stage ignition indirectly indicates the uniformity of the reacting mixture and homogenous ignition. It is further noted that, although ignition delay times have traditionally been the primary data reported from RCM experiments, other fundamental quantities such as intermediate species concentrations can also be measured. Speciation measurement techniques conducted in RCM experiments will be discussed later.

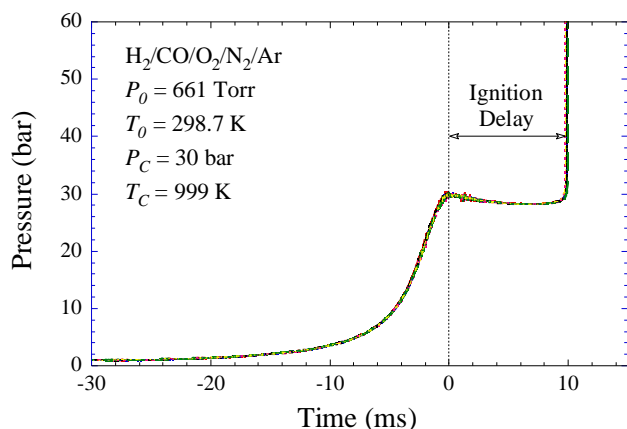


Fig. 2(a) – Pressure trace illustrating the ignition and repeatability of seven experiments for a  $\text{H}_2/\text{CO}$  mixture. Molar composition:  $\text{H}_2/\text{CO}/\text{O}_2/\text{N}_2/\text{Ar} = 9.375/3.125/6.25/18.125/63.125$ . Initial conditions –  $T_0 = 298.7$  K and  $P_0 = 661$  Torr. Conditions at the end of compression –  $T_C = 999$  K and  $P_C = 30$  bar.

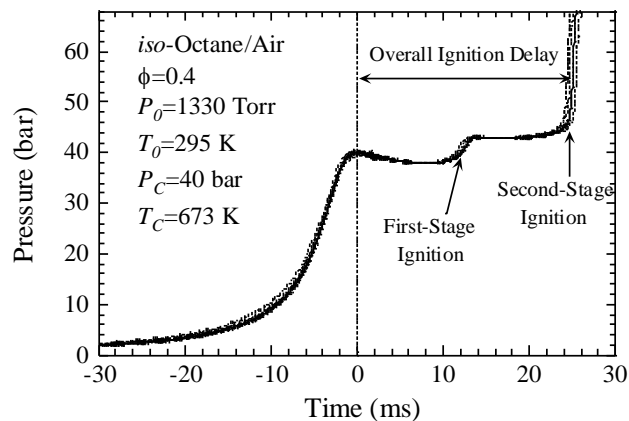


Fig. 2(b) – Demonstration of experimental repeatability for auto-ignition of an *iso*-octane/air mixture under conditions of two-stage ignition. Conditions:  $\phi = 0.4$ ,  $P_0 = 1330$  Torr,  $T_0 = 295$  K,  $P_C = 30$  bar, and  $T_C = 673$  K.

## 2.2. Effect of Fluid Mechanics and Temperature Homogeneity inside an RCM

Due to the high piston velocities during the compression event, complex fluid mechanics features can affect the state of the reacting core in the reaction chamber. Interpretation of RCM data in the literature has been difficult because of temperature inhomogeneity within the reaction chamber and the lack of heat loss characterization for the associated experiments. It has been observed that data obtained in different RCMs, even under similar conditions, can be

quantitatively different [e.g., 23–27]. These discrepancies are partly attributable to different heat loss characteristics after the end of the compression stroke and are partly attributable to the difference in fluid mechanics effects between various machines. Various studies [e.g., 21,28–30] have shown that the motion of the piston during the compression stroke creates a roll-up vortex, which results in mixing of pockets of cold gas from the boundary layer with the hot gases in the core region. The lower section of Fig. 3 depicts the creation of a roll-up vortex due to piston motion using flat pistons, while the upper section of Fig. 3 illustrates how the boundary layer can be contained using a properly-designed creviced piston. The creation of a roll-up vortex produces undesired mixing of cold boundary layer gas with hotter core gas and leads to difficulties in accurately characterizing the state of the reacting mixture. As a result of the roll-up vortex, there is an inhomogeneous temperature field in the reaction chamber and reaction will proceed to different extents at different locations depending on the local temperature.

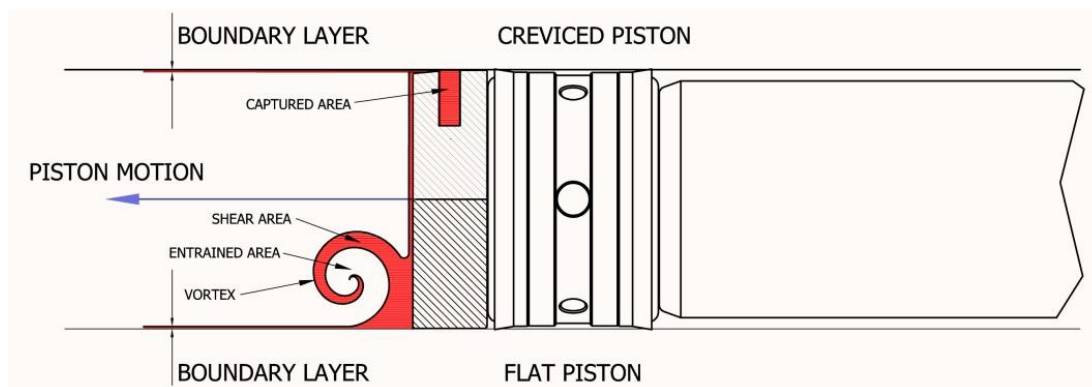


Fig. 3 – Illustration of creation of roll-up vortex due to piston motion during the compression stroke (lower section) and containment of boundary layer through a crevice (upper section) through proper design.

The effect of fluid mechanics is particularly more complicated and difficult to detect because it does not significantly affect the pressure trace and it may lead to significant temperature gradients, and ultimately, to the failure of the adiabatic core hypothesis. If the aerodynamic effect becomes significant and the adiabatic core hypothesis fails, there is no easy way to determine the temperature inside the reaction chamber. As a result, unambiguous determination of the state of the reacting mixture and systematic characterization of the resulting flow field inside an RCM are important in order to obtain reliable kinetic data from RCMs and to bridge the problem of reconciling data taken from different machines.

Several studies have contributed to the understanding of the fluid mechanics and temperature field inside an RCM, by both computational fluid dynamics (CFD) calculations and experimental measurements. Griffiths *et al.* [21] numerically showed that the hot core region generated at the end of compression is virtually isentropic and spans approximately 70% of the volume of the combustion chamber at the end of compression in their facility. The differences observed between computational results using spatially uniform conditions (i.e. zero-dimensional modeling, see below) and CFD simulation were attributed to the effect of the temperature gradient that was accounted for in the CFD analysis [21].

In the study of Clarkson *et al.* [30], the temperature field was imaged by Rayleigh scattering and laser induced fluorescence (LIF) of acetone in their RCM. Acetone-LIF was found to nicely



characterize the temperature variations in the RCM whereas Rayleigh scattering was relatively less sensitive [30]. It was observed experimentally that the roll-up vortex had penetrated the center of the combustion chamber at the end of compression [30]. The temperature difference between the hot gases and the roll-up vortex was estimated to be 50 K [30]. Furthermore, LIF of acetone generated by the decomposition of di-*tert*-butyl peroxide unambiguously showed the temperature stratification at the center of the reaction chamber [30].

Griffiths *et al.* [31] investigated temperature and concentration fields in a rapid compression machine by using a number of experimental techniques, including Schlieren photography, planar laser induced fluorescence (PLIF) of acetone, PLIF of formaldehyde, and chemiluminescence imaging. In order to illustrate the interaction of chemistry with the temperature field in the RCM, Griffiths *et al.* [31] contrasted the combustion behavior of di-*tert*-butyl peroxide with that of *n*-pentane. The overall reaction of the former is characteristic of thermal ignition, while the combustion of the latter was investigated in the compressed temperature range exhibiting a negative temperature dependence of the overall reaction rate. With imaging taken up to 10 ms after the end of compression, results showed that the di-*tert*-butyl peroxide reaction proceeded faster in the zone of peak temperature [31]. A somewhat similar behavior was observed for *n*-pentane combustion when the compressed temperature was at the lower end of the NTC range [31]. By contrast, at compressed temperatures close to the upper end of the NTC region, the reaction in the cooler zone developed faster and the temperature inhomogeneity inside the reaction chamber rapidly smoothed out [31]. Griffiths *et al.* [32] further used chemiluminescence imaging together with filtered Rayleigh scattering in an RCM to characterize the transition from non-knocking to knocking reaction and the evolution of the spatial development of the reactivity. At compressed temperatures outside the NTC region, the presence of temperature inhomogeneity leads to the onset of ignition occurring in the highest temperature region [32]. In contrast, the effect of the NTC dependence of reaction rate is to smooth out the temperature inhomogeneity inside the reaction chamber [32].

Desgroux *et al.* [22,33] made direct measurements of temperature in an RCM using a thermocouple and single point Rayleigh scattering. These measurements confirmed the existence of an adiabatic core gas at the end of compression. Desgroux *et al.* [33] also conducted fine wire thermocouple measurements for non-reactive and reactive mixtures at different radial locations. They observed a uniform temperature field for a few milliseconds after the end of compression and the subsequent development of temperature inhomogeneity due to heat loss to the wall and to gas recirculation [33]. For non-reactive mixtures the temperature inhomogeneity persisted after compression, whereas for reactive *iso*-octane mixtures, the spatial temperature inhomogeneities were smoothed out as the ignition was approached, which the authors ascribed to the negative temperature coefficient of reaction rate [33].

Recognizing that the proper characterization of fluid mechanics, temperature, and pressure within the reaction chamber of an RCM is important for reliable data interpretation and consistent comparison with models, significant contributions have been made to establish a well-defined homogeneous zone within an RCM. The addition of a crevice into the side of the piston can potentially eliminate the complicated fluid mechanics and the unwanted mixing with near-wall cold gases inside the combustion chamber, resulting in a more homogeneous mixture [cf. 29]. A unique sabot design to achieve the same purpose has also been demonstrated [17]. These features have made possible more accurate characterization of mixture temperature for kinetic studies.

Würmel and Simmie [26] carried out a CFD study of an RCM reaction chamber using a dual-opposed-piston system to test the effect of suppressing boundary layer roll-up by capturing the boundary layer using a creviced piston configuration. Figure 4 shows a comparison of the predicted temperature fields at approximately 10 ms after the end of compression using flat and creviced piston head designs [27]. It is clear that using a creviced piston design leads to a much more homogeneous temperature field throughout the reaction chamber.

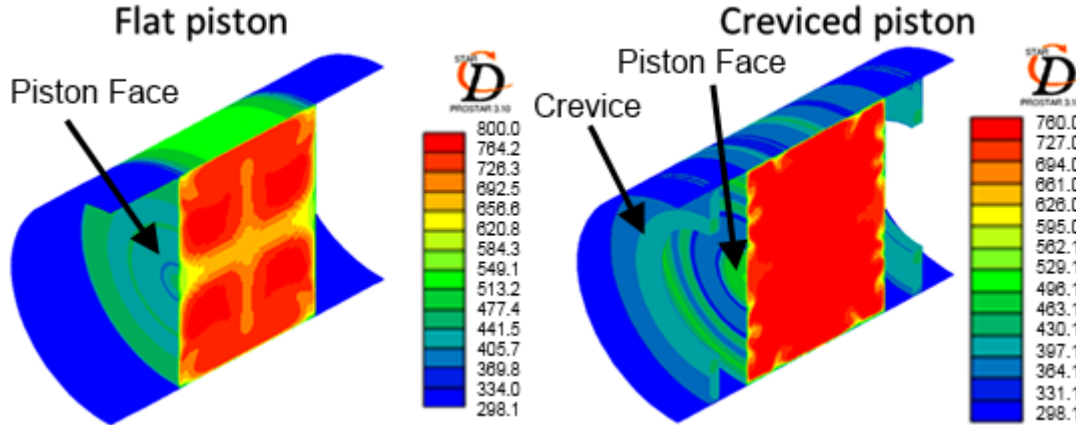


Fig. 4 – Comparison of predicted temperature fields at 26.4 ms from the start of compression (with a compression time of approximately 16 ms) for N<sub>2</sub> gas at  $T_0 = 298$  K and  $P_0 = 0.5$  bar using flat and creviced piston head designs [27].

Several studies have attempted to optimize the crevice design for particular operating conditions. In the work of Mittal and Sung [16], simulations were conducted by systematically varying different dimensions of the piston head to investigate their individual and combined effects on vortex suppression. The insights gained from the simulations included: (1) the total volume of crevice should be large enough to completely contain the boundary layer; (2) the crevice entrance should be large enough to allow the boundary layer to flow into the crevice, but not so large as to cause flow circulation within the crevice inlet; (3) increasing the length of the crevice inlet does not affect the fluid mechanics of the core region in any way, but the gas in the crevice is cooler due to increased heat loss from the crevice entrance; (4) there exists a critical dimension at the end of the crevice inlet, beyond which the undesirable back flow from the crevice to the main cylinder volume occurs. Based on the simulated results, the final piston head configuration was optimized and selected under the desired operating conditions [16]. In the CFD simulations of Würmel and Simmie [26], the piston head crevices were optimized for the twin-piston RCM, in terms of volume, location, and the dimension and geometry of the channel connecting the crevice and the chamber. Furthermore, Würmel and Simmie [26] observed similar trends with respect to crevice design as the work of Mittal and Sung [16] described above. These similarities were noted despite some differences in modeling techniques, including the fact that Mittal and Sung [16] considered laminar flow while Würmel and Simmie [26] considered a  $k-\epsilon$  model. The channel connecting the crevice and the chamber was optimized and the ideal geometry was found to be rectangular [26]. An angled channel design was seen to help somewhat in the cooling of the trapped gas in the piston head crevice.

To compare the effectiveness of creviced-piston versus flat-piston designs in suppressing the roll-up vortex, acetone-PLIF measurements were conducted for both creviced piston and flat

piston head designs [34]. It is worth noting that the crevice configuration of this particular RCM was chosen with the aid of numerical simulation [16] as discussed previously. The acetone fluorescence signal can be highly sensitive to temperature for certain excitation wavelengths. For instance, at 279 nm excitation and constant acetone fraction, the associated acetone fluorescence signal is decreased by 42% as the temperature increases from 600 K to 800 K. Figure 5 compares the PLIF images at 2 ms post compression for both flat- and creviced-piston heads, along with the associated photon count profiles integrated along the width of the laser sheet and the deduced temperature distributions. It is also noted that the bore of the reactor cylinder is 2 inches (5.08 cm) and the end of the chamber is fitted with a quartz window, which provides full view of the combustion chamber for fluorescence imaging [34]. The pressure at the end of compression was kept constant at 39.5 bar when comparing both piston head configurations and a relatively high compression ratio was used. In Fig. 5, the gray line is the actual fluorescence signal, while the dashed line represents the ideal exponential decay of the fluorescence intensity that would be observed in a uniform temperature field. In addition, the red line denotes the deduced temperature profile. A radial dimension equal to 0 corresponds to the central axis of the cylindrical chamber and 2.54 cm and  $-2.54$  cm respectively represent the cylinder wall on either side. Note that the temperature drops sharply at the boundaries of the cylinder (2.54 cm and  $-2.54$  cm); this is due to the cold boundary layer at the chamber walls.

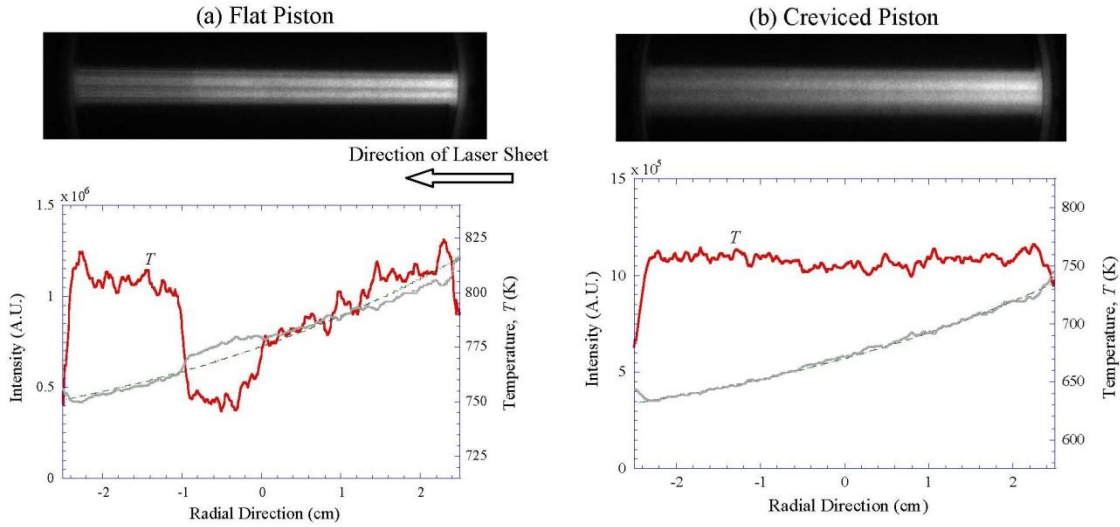


Fig. 5 – PLIF image, integrated fluorescence intensity profile (gray line), and deduced temperature (red line) at 2 ms post end-of-compression. Dashed line represents fluorescence intensity as in a uniform temperature field. (a) Flat piston with pressure of 39.5 bar at the end of compression. (b) Creviced piston with pressure of 39.5 bar at the end of compression. Laser sheet enters from the right side of the image.

It should be noted that any increase in the fluorescence signal corresponds to a reduced temperature and any depression indicates an increase in temperature. For the case of the flat piston, Fig. 5(a) shows a distinct enhancement of fluorescence intensity at the center of the chamber; this corresponds to a reduction of approximately 65 K in temperature and indicates a sharp temperature gradient therein. Hence, the flat piston design leads to significant mixing of the cold vortex with the hot core region, which causes alternate hot and cold regions inside the reaction chamber, consistent with the picture provided in Fig. 4 by the CFD calculations of

Würmel [27]. On the other hand, for the creviced piston an almost exponentially decaying fluorescence signal is shown in Fig. 5(b), as would be observed in a uniform temperature field. These tests demonstrate that the creviced piston head is indeed successful in suppressing the vortex roll-up, leading to a more uniform temperature field. At subsequent time steps, even up to 114 ms after the end of compression, there is no effect due to the vortex [34], as shown in Fig. 6. Eventually, the effect of the vortex becomes noticeable, e.g., the depression due to the vortex was approximately 40 K at 200 ms even for the creviced piston [34]. It was also noted in [34] that the effect of the vortex roll-up is significantly reduced as the pressure is increased because of the diminishing boundary layer thickness due to smaller thermal diffusivity. Therefore, caution needs to be exercised when performing RCM experiments below the pressure used to optimize the creviced piston head configuration.

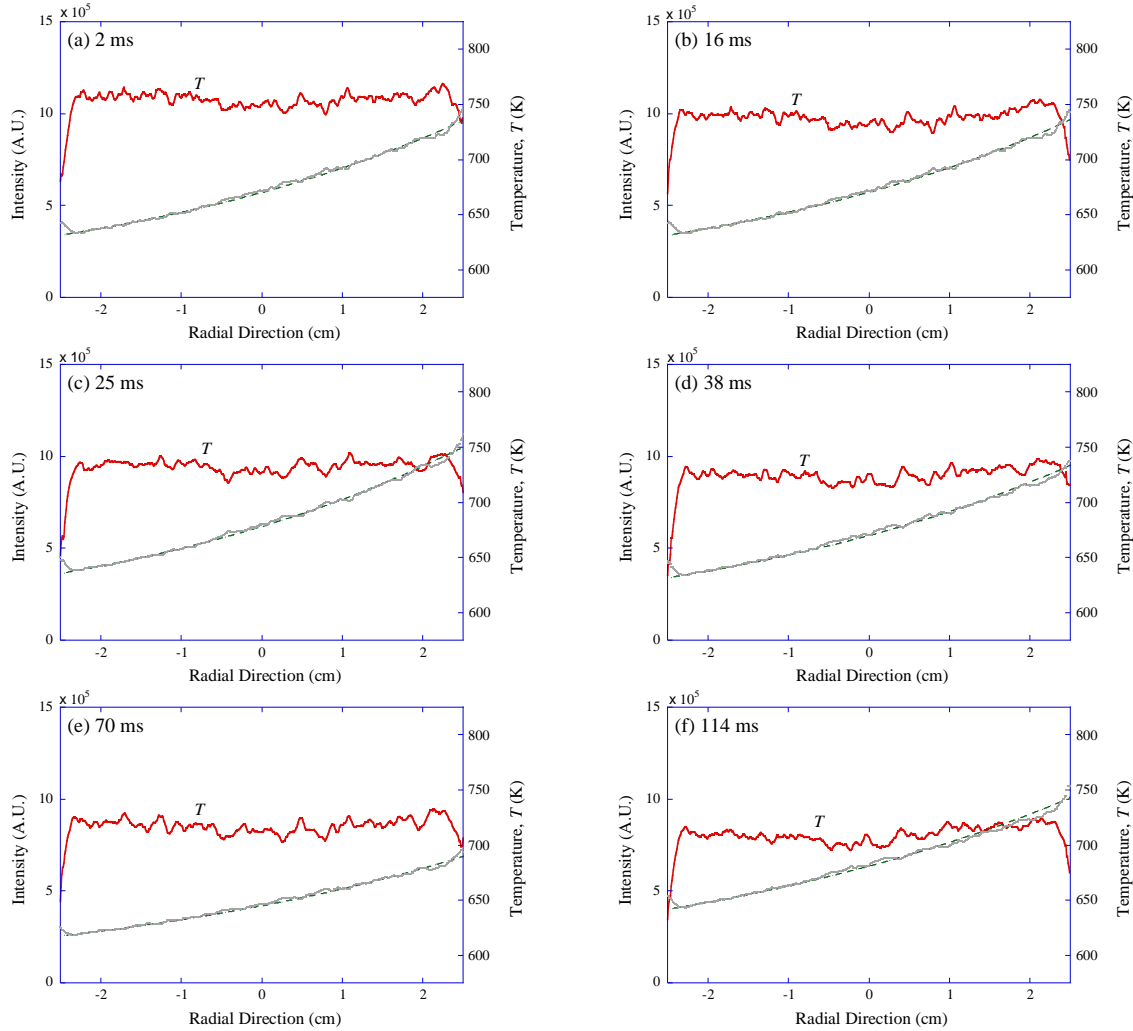


Fig. 6 – PLIF intensities and deduced temperature distributions at varying post end-of-compression times for a creviced piston head. Gas composition: 1% acetone in nitrogen. Conditions at the end of compression: pressure=39.5 bar and temperature=770 K. Gray line: raw fluorescence intensity. Dashed line: calculated fluorescence intensity in a uniform temperature field by using the Beer-Lambert law. Red line: deduced temperature distribution.

In addition to the pressure dependence, the effectiveness of a creviced piston head in suppressing the vortex effect can also be affected by the test gas. In their CFD study, Würmel and Simmie [26] observed a strong dependence of the crevice performance on the test gas used. Specifically, although an optimal crevice was identified for test gases such as nitrogen, oxygen, and argon, it was not possible when using helium, due to helium's high thermal diffusivity and associated high heat loss. Differences in heat losses from different test gases are due to differences in their thermal diffusivities; species with high thermal diffusivities show greater heat losses.

Although the use of creviced pistons has been shown to effectively suppress the effect of the roll-up vortex, computational studies have also demonstrated that it can introduce some other multi-dimensional effects during multi-stage ignition [35,36]. This in turn can affect the fidelity of zero-dimensional modeling for adequate interpretation of experimental data, and can significantly influence quantitative species sampling [36,37] because of the relatively large crevice volume. These undesirable effects are due to mass transfer between the crevice and the reaction chamber, which can potentially be overcome with crevice containment [17,36–39]. The principle of crevice containment is to separate the crevice from the main reaction zone by a seal that is engaged only when the piston reaches the end of compression. As such, the crevice is connected to the main chamber and avoids the formation of the roll-up vortex during the compression stroke, while during the post-compression period the crevice and the main reaction chamber are separated to avoid the flow of additional mass into the crevice when chemical heat release takes place in the reaction chamber. Recent experimental work implementing the concept of crevice containment in RCM demonstrated a significant reduction in the post-compression pressure drop [38,39]. Further experimental studies are warranted to explore the benefits of incorporating crevice containment into existing RCMs, especially for multi-stage ignition response.

Although RCM designs remain varied and are still evolving as new RCMs are built, key design objectives include a well-defined core region, fast compression, the ability to vary the stroke and clearance (i.e. compression ratio), optical accessibility, capability for species measurement, and minimum mechanical vibrations. In addition, it is important to carry out systematic experimental and computational characterization of an RCM in order to assess its performance in terms of vortex formation and temperature homogeneity inside the reaction chamber over a range of operating conditions, such as stroke length, clearance volume, compressed gas pressure, temperature, etc. [40]. The individual and combined effects of these factors can significantly affect the formation of the roll-up vortex. A good understanding of the performance of an individual RCM over the associated range of operating conditions is critical to obtain reliable chemical kinetics data.

### **3. Interpretation of RCM Data**

#### *3.1. Facility Effect and Heat Loss Characterization*

As discussed above, the ability for fast compression and vibration-free piston stopping are prime requirements of an RCM. In addition, the existence of a thermodynamically well-defined core region of the compressed gas is essential. In Eq. (2), everything except  $T_c$  is a measured parameter; therefore, with the known temperature dependence of  $\gamma$ ,  $T_c$  can be determined by numerical integration. After the end of compression, if the assumption of an adiabatic core is assumed to hold, the temperature evolution can also be determined from the measured pressure.

The assumption of an adiabatic core will hold if the effect of heat loss is indeed limited to the boundary layer. However, if the fluid mechanics effects due to vortex roll-up and mixing become substantial, the adiabatic core hypothesis will break down and there will be ambiguity in determining the temperature of the reacting mixture. From a kinetic study point of view, the accurate determination of temperature is of prime importance due to the exponential dependence of the reaction rate on temperature. Again, it is important that any RCM design should minimize the effect of roll-up vortex and establish the validity of the adiabatic core hypothesis before reliable experimental data can be obtained. Thus, the existence of a thermodynamically well-defined homogeneous reactant mixture is the key to obtaining meaningful data from an RCM.

Assuming a homogeneous reactive mixture can exist within the reaction chamber, Fig. 7 illustrates a simplistic view that an RCM experiment represented by an ideal constant volume autoignition perturbed by the associated facility effect due to the compression stroke and the heat loss from the core region to the walls of the reaction chamber. Plotted in the facility effect graph, Fig. 7(a), is the measured pressure for a non-reactive mixture divided by the pressure at the end of compression. We see that during compression this normalized value is a fraction and reaches one at the end of compression. Thereafter, it is lower than unity due to facility effects, mainly caused by heat losses of the compressed gas to the walls of the machine. Plotted in the chemistry graph, Fig. 7(b), is the normalized pressure calculated in an adiabatic, constant volume simulation for a reactive mixture with initial conditions of  $P_C$  and  $T_C$ . For an RCM autoignition experiment, the observed pressure trace would be a result of combining Figs. 7(a) and 7(b), in which chemical reaction tends to negate the pressure drop due to the facility effect, with a rapid rise in pressure due to autoignition of the charge at some post end-of-compression time that is defined as the corresponding ignition delay time.

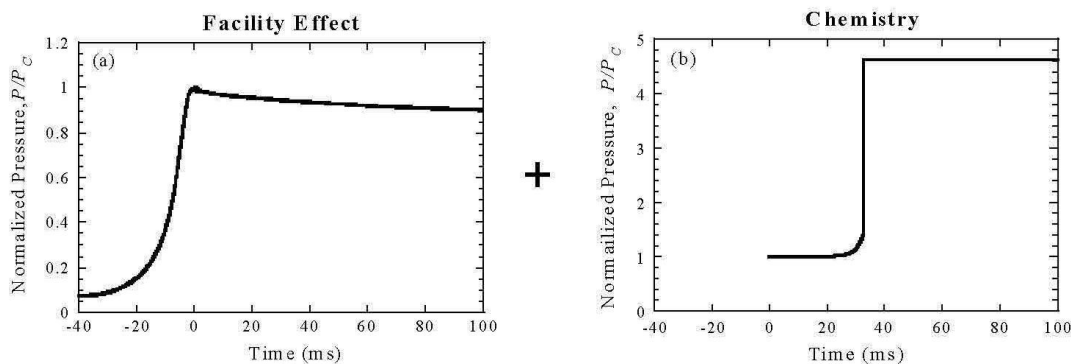


Fig. 7 – Simulating reactive RCM experiment by combining (a) the facility effect (compression stroke and heat loss) and (b) the chemical kinetics in an adiabatic constant volume reactor.

Therefore, a numerical model that accounts for the compression stroke and the effect of heat loss is needed to simulate an RCM experiment. There are typically two approaches used in RCM modeling to consider the effect of heat loss after reaching the end of compression. One approach is to include a heat loss term in the energy equation while keeping the reactor volume constant [e.g., 41,42], while the other is to specify a volume expansion term while applying the adiabatic core assumption [e.g., 43]. For the former approach, an empirical parameter in the heat loss term is used and varied in order to match the simulated pressure trace with the experimental data. The rationale behind the latter approach is that, as the near-wall boundary layer cools during the post end-of-compression period, the core gas away from the boundary layer experiences an effective

volumetric expansion even though the geometric volume of the reaction chamber remains the same after reaching the end of compression. Moreover, when the roll-up vortex is effectively suppressed (e.g., by using a creviced piston), the effect of heat loss on the core gas occurs only through this expansion. As such, the experimental pressure trace can be used to calculate the time-dependent “effective volume” of the core region.

Both of the abovementioned approaches can be used to simulate and match the experimental pressure history. However, the two approaches lead to different temperature histories during the post end-of-compression period. Based on a CFD simulation of a non-reactive RCM experiment with N<sub>2</sub> gas [cf. 16,34], the resulting post end-of-compression temperature profiles using the two different approaches are compared. The initial conditions specified in the simulation were N<sub>2</sub> at rest at an initial temperature of 297 K and at an initial pressure of 260 Torr. Figure 8 shows the time evolution of the pressure and the maximum instantaneous temperature in the chamber obtained from the CFD calculations, with time = 0 representing the end of compression. Again, both the pressure and the maximum temperature decrease with time during the post end-of-compression period because of heat loss. In order to highlight the difference in the temperature histories deduced from the two approaches, both approaches were assumed to predict the same  $P_C$  and  $T_C$  as well as matching the post end-of-compression pressure trace obtained from the CFD calculation. For the approach of including a heat loss term in the energy equation, the ideal gas law is applied to determine the post end-of-compression temperature based on:  $T(t)=T_C [P(t)/P_C]$  due to constant reactor volume. With the approach of “effective volume”, the time dependent temperature profile can be deduced using the adiabatic core hypothesis:  $T(t)=T_C [P(t)/P_C]^{(\gamma-1)/\gamma}$ , or the ideal gas law,  $T(t)=T_C [P(t)/P_C][V(t)/V(0)]$ , where  $V(t)$  is the time varying effective volume. For the two deduced temperature histories compared in Fig. 8, it is seen that the approach of including a heat loss term leads to a much lower temperature history even though the pressure histories are identical. This is because in this approach heat loss is implicitly assumed to be throughout the entire volume of the combustion chamber and not just within the boundary layer. Furthermore, Fig. 8 shows that the temperature deduced from the approach of “effective volume” matches exactly with the maximum temperature obtained from the CFD calculation for long duration. Through this example, the approach of “effective volume” for simulating RCM experiments is computationally validated.

To prepare for the simulation of a given reactive mixture in an RCM experiment, a non-reactive experiment is first carried out using a mixture with the same values of heat capacity, initial pressure, and initial temperature as for the reactive mixture, typically by replacing O<sub>2</sub> with N<sub>2</sub>. Based on the non-reactive pressure trace, the approach outlined in [16] for characterizing the effective volume is as follows. For the compression stroke, an empirically-determined parameter is added to the actual time-dependent geometric volume of the combustion chamber in order to match the simulated pressure with the experimental value measured at the end of compression. Hence this empirical parameter simulates the heat loss during the compression period. After the end of compression, the volume expansion is specified in terms of a polynomial fit to determine the effective volume after compression, according to the adiabatic core assumption. Alternatively, rather than reporting polynomial fit parameters or providing subroutines for modelers to integrate into the variable volume simulations, the effective volume history can be calculated by Eq. 3 and reported in tabular format, as employed in [44,45].

$$V(t) = V_0 \left( \frac{P(t)}{P_0} \right)^{\frac{1}{\gamma}}, \quad (3)$$

The measured pressure history from the non-reactive experiment is directly converted into a volume history using the mixture specific heat ratio (as a function of temperature) and the adiabatic core relations. There are several advantages associated with the volume history tabulation approach, including that it is simpler to implement in Chemkin-type simulations, it provides close agreement with experimental pressure profiles, and it avoids divergence of the polynomial function when the calculation time exceeds the fitting range.

Neither of these methodologies to calculate the effective volume trace is able to account for the effect of heat release due to exothermic reactions. For simulating experiments exhibiting two-stage ignition phenomena, the same effective volume trace is used before and after the first-stage ignition event. The effect of this omission will be discussed in Section 3.4.

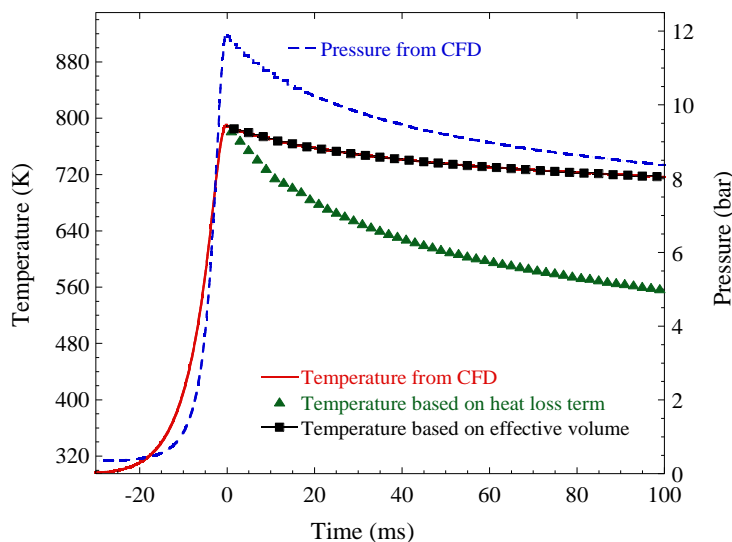


Fig. 8 – Comparison of CFD-determined RCM results with the deduced post end-of-compression temperature histories using two different approaches: (1) including a heat loss term in the energy equation and (2) using effective volume of core region. Test gas was  $N_2$ , initially at rest, with initial pressure and temperature of 260 Torr and 297 K, respectively. The  $P_C$  and  $T_C$  are  $\sim 12$  bar and  $\sim 800$  K, respectively.

### 3.2. Effect of Compression Stroke

Figure 9 illustrates an example of an RCM simulation using dimethyl ether (DME) mixtures [46]. Experimental and simulated pressure traces for both the reactive and the corresponding non-reactive mixtures with the same specific heat ratio are shown and compared in Fig. 9. As explained above, based on the pressure history of the non-reactive experiment, the parameters required for the heat transfer model (i.e. the effective volume parameters) are deduced. The experimental and computed pressure traces for the non-reactive mixture are seen to match very well for both compression and post end-of-compression events, indicating the adequacy of the present heat transfer model. The empirically-determined parameters are then used to simulate the corresponding reactive case. Furthermore, the present heat loss modeling approach ensures that along with the pressure history, the temperature history of the adiabatic core, is also correctly simulated. Compared to the experimental data, the simulated pressure trace obtained using the particular model used in [46] at the condition of the experiment shown in Fig. 9 over-predicts the



first-stage and total ignition delay times. Mittal *et al.* [47] used a detailed chemical kinetic mechanism to simulate ignition delay times measured in an RCM for syngas mixtures and found they were able to accurately reproduce these data by treating the pressure drop after compression as an adiabatic expansion process using the procedure discussed here. Furthermore, a computational study of H<sub>2</sub> ignition in an RCM [48] showed that zero-D simulations in conjunction with the approach of “adiabatic volume expansion” performs very well in adequately predicting the ignition delay, as compared with the results obtained by CFD simulations, although pressure rise rates could be different for some cases.

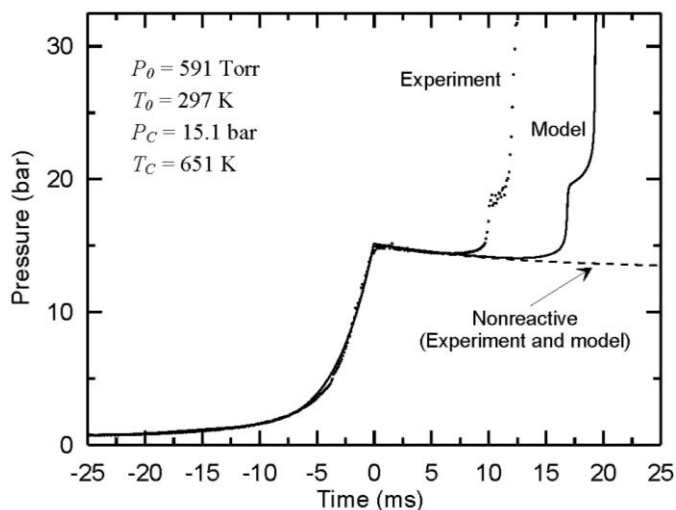


Fig. 9 – Experimental and simulated pressure traces for a mixture with molar composition of DME/O<sub>2</sub>/N<sub>2</sub>=1/4/30. Both reactive and nonreactive conditions are shown.

For the reactive RCM experiments, the pressure trace during the compression stroke is typically said to have insignificant reactivity (i.e. a lack of exothermic or endothermic effects during the compression stroke) if it does not diverge from the non-reactive pressure trace prior to the end of compression. However, during the compression stroke, radical initiation processes begin to occur that can subsequently play a role in the further development of the radical pool after compression. Therefore, even though there is little overall chemical reaction during compression, the ignition processes observed thereafter may be responsive to chemistry occurring during the compression stroke. Such chemistry effects can be included in the modeling approach discussed above, as predictions are calculated based upon the initial conditions prior to compression and the pressure history, corrected for heat loss, over the entire experiment.

To demonstrate the effects of small radical production during compression, model results of DME/oxidizer mixtures [46] are presented in Fig. 10 using two different modeling constraints: (1) the entire compression and post end-of-compression processes are simulated using the initial experimental mixture conditions; (2) only post-compression processes are simulated using the thermodynamic state at the end of compression (i.e.  $P_C$  and  $T_C$ ) as the initial pressure and temperature, and the initial experimental reaction mixture composition. While the effect of heat loss (deduced from the respective non-reactive counterpart) is accounted for in both calculations, the two predictions can differ significantly in computed ignition delay following compression, especially for experimental conditions that result in short ignition delays. For example, from Fig. 10, at compressed conditions of 20.1 bar and 639 K, the two modeling approaches yield ignition

delays of 31.87 ms for (1) and 34.31 ms for (2), which is approximately a 7% difference. At 720 K, however, these values are 2.34 ms and 3.69 ms, respectively, which is almost a 60% difference. From the time histories of important radicals in the DME system (i.e. H, O, OH, HO<sub>2</sub>, CH<sub>3</sub>) during and after the compression stroke shown in [46], these radicals are all present in sub-ppm (i.e. HO<sub>2</sub>, CH<sub>3</sub>) and sub-ppb (i.e. H, O, OH) levels at the end of compression. The radical pool developed during compression, however small, can have a marked effect on characteristic ignition delay times observed for the pressures and temperatures studied here, simply because chemical induction processes have characteristic times that are comparable to the observed ignition delay times at these conditions. These results also demonstrate the importance of including the compression stroke in simulations when comparing with the experimental data.

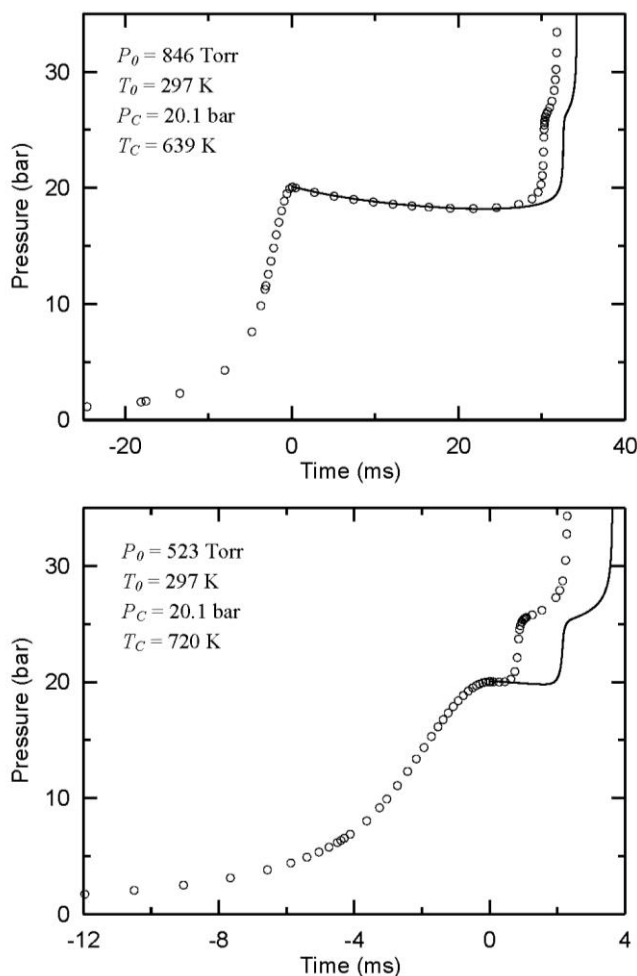


Fig. 10 – Effect of the compression stroke on modeled pressure traces for a DME/O<sub>2</sub>/N<sub>2</sub> mixture (1/4/30 molar composition). Open symbols represent calculations performed considering the RCM compression stroke; lines are results obtained by initializing the calculations at the end of compression for the compressed pressure and temperature conditions listed and using the initial mixture composition. The heat loss effect is included in both calculations.

The discussion above indicates that chemical induction processes are influenced by even small perturbations in the initial radical pool formed during compression. This result supports the views of [49,50] put forth in analyzing the reported discrepancies between chemical kinetic

predictions and experiments of syngas/air ignition delay times. Some rapid compression studies have simulated their experiments as constant volume processes using conditions at the end of compression [41] or experimentally determined effective pressures and temperatures [51,52] as initial reference parameters. These investigations [41,51] reported small differences (within experimental uncertainty) in computed ignition delay times between these approaches and ones that include compression and post end-of-compression simulations. However, the validity of modeling rapid compression experiments in this manner should always be verified since, as shown above, this can lead to considerable differences.

### 3.3. Comparison of Shock Tube and RCM Data

Due to the time scales involved in RCMs (from approximately 5–100's of ms) and shock tubes (from  $\mu$ s to approximately 10 ms), it is advantageous to use both facilities in a complementary way to measure ignition delay times across a wide temperature range. These ignition delay times typically depend on the temperature of an experiment, where generally higher temperatures lead to shorter ignition delay times, except in the NTC region. Thus, combining both facilities permits the study of fuels in the temperature range of approximately 600–2000 K.

Figure 11 is an example of using both facilities to measure ignition delay times for a natural gas mixture in the temperature range of 950–1550 K, and at pressures of approximately 10 and 20 atm [53]. The shock tube data are recorded at higher temperatures (1160–1470 K), where the ignition delay timescale ranges from approximately 40  $\mu$ s to 2 ms, whereas the RCM data are recorded at lower temperatures (950–1100 K), where the ignition delay timescale ranges from approximately 3 to 100 ms.

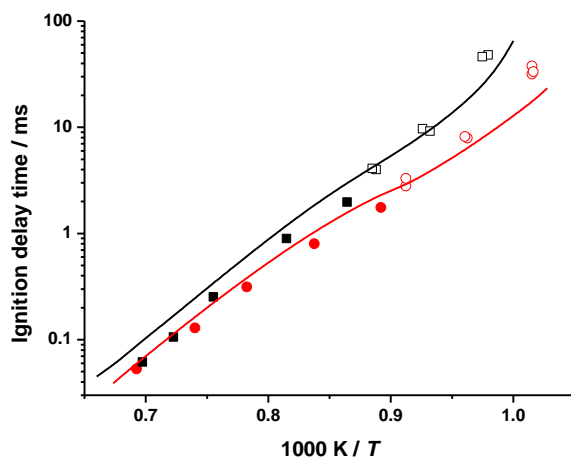


Fig. 11 – Ignition delay times indicating the complementary nature of RCM and shock tube measurements for a natural gas mixture of 81.25% CH<sub>4</sub>, 10% C<sub>2</sub>H<sub>6</sub>, 5% C<sub>3</sub>H<sub>8</sub>, 2.5% C<sub>4</sub>H<sub>10</sub>, and 1.25% C<sub>5</sub>H<sub>12</sub> at  $\phi = 0.5$  in air [53]. Symbols are experimental results;  $\square$  RCM 10 atm,  $\blacksquare$  ST 8 atm,  $\circ$  RCM 20 atm,  $\bullet$  ST 19 atm. Lines are model predictions.

As has been shown, due to the wide range of test times in an RCM, it is necessary to consider facility effects such as reaction during compression and heat loss after compression when performing simulations. It is also important to consider facility dependent effects when

directly comparing ignition delay times measured in different RCMs or between RCMs and shock tubes. To illustrate this point, Fig. 12 compares ignition delay times measured in an RCM by Gallagher *et al.* [54] for a propane/‘air’ mixture at  $\phi=0.5$ , and  $P_C=30$  atm together with shock tube data taken under similar conditions in two different shock tubes, one by Herzler *et al.* [55] and the other by Petersen *et al.* [56]. It can be seen that at 850 K ( $1000/T \approx 1.15$ ), there is almost two orders of magnitude difference between the ignition delay times measured in the RCM [54] and those measured in the shock tube by Herzler *et al.* [55]. This problem has been discussed in the work of Petersen *et al.* [56] and also in the review by Davidson and coworkers [57,58]. The discrepancy can be ascribed to differences in facility dependent effects.

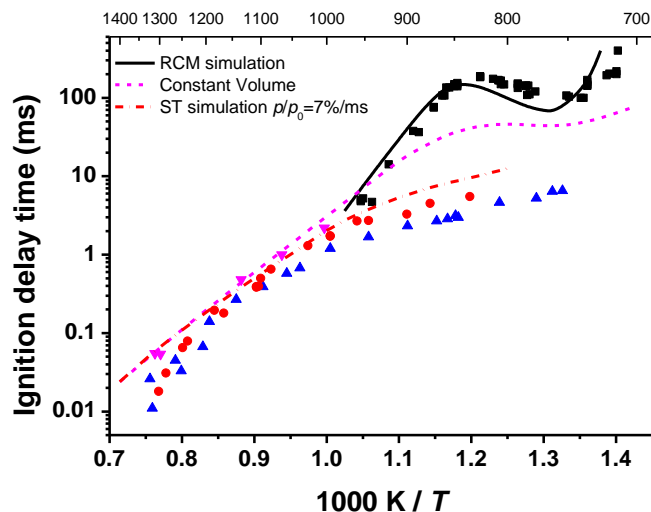


Fig. 12 – Propane ignition delay time measurements at low temperatures and high pressures for fuel in ‘air’ mixtures at  $\phi = 0.5$ ,  $P_C = 30$  atm, ■ [54], ● [55] in  $N_2$ , ▲ [55] in Ar, ▼ [56] and comparison with a traditional constant energy and volume (or density) simulation and with a simulation using  $dP/dt = 7\%/ms$ , all using the mechanism of Gallagher *et al.* [54].

In an RCM, there are competing facility-dependent effects that influence the ignition delay time, namely the radical pool buildup during the compression stroke and the post end-of-compression heat loss. For short ignition delay times, the radical pool buildup dominates the heat loss effect, and the ignition delay time could be shorter than a corresponding case that does not consider the compression stroke. However, for long ignition delay times, the heat loss effect would dominate over the radical pool effect and the measured ignition delay times would be longer than a corresponding case that does not consider the facility dependent heat loss. By contrast, Davidson and coworkers [57,58] have shown that shock tubes can show a nearly constant rate of pressure rise as a function of time due to non-ideal facility-dependent behavior, and observed a  $dP/dt$  of 2%/ms for hydrogen-oxygen experiments in their shock tube. This effect tends to make the measured ignition delays shorter than a corresponding case that does not consider the facility dependent pressure rise as temperature will rise with pressure. Thus, the facility dependent effect on long ignition delay times is opposite when comparing shock tube and RCM ignition delays, and as ignition times get longer, the apparent difference between ignition delays measured in shock tubes and RCMs will tend to diverge. A naïve comparison of the ignition delay times might mistakenly conclude that the experiments are irreconcilable. Yet this is not the case, based on a proper comparison.

As emphasized earlier for modeling RCM experiments, one needs to simulate both the compression phase to include any reaction during compression and the post end-of-compression phase to account for heat losses. Figure 12 further shows a comparison of such a simulation of RCM experiments using a propane mechanism developed by Gallagher *et al.* [54], where reasonable agreement can be observed between the simulations and experiments. Also plotted on this same graph is a simulation assuming adiabatic, constant volume conditions. At temperatures below approximately 950 K, the adiabatic simulations predict faster ignition times compared to the RCM ones, due to the lack of heat loss after compression, but at temperatures above 950 K, the RCM simulation is slightly faster than the adiabatic, constant volume case because it includes reaction during compression, and thus allows the chemistry to develop. For the shock tube results [55,56] shown in Fig. 12, it can be seen that, at temperatures below approximately 1100 K, the measured ignition delay times are considerably faster than those predicted using an adiabatic, constant volume simulation. For comparison, Fig. 12 also shows a simulation assuming a  $dP/dt$  of 7%/ms and demonstrates that this assumption agrees better with the lower temperature shock tube ignition delay data compared to the adiabatic, constant volume simulations. However, it still does not capture the experimental data, and it is clear in the publication by Petersen *et al.* [56] that the pressure rise prior to ignition is not a constant  $dP/dt$  but is instead a much greater pressure rise prior to fuel autoignition due to some unknown phenomenon. Thus, by comparing each experiment to the correctly modeled simulations, it is found that the agreement with the model is reasonable, even though the direct agreement between the measured ignition delays is very poor. These effects were also discussed in a publication by Chaos and Dryer [59], in which they ascribed them to be, at least in part, due to fluid dynamic non-idealities as well as deflagrative processes typical of mild ignition events. These effects were not only discussed for syngas mixtures, but also for hydrocarbon fuels including *iso*-octane, toluene, and *n*-decane. Chaos and Dryer [59] concluded that a proper characterization of each facility is needed in order to help generate an accurate chemical kinetic model for the combustion of any fuel.

### 3.4. Adequacy of Zero-Dimensional Approach in RCM Modeling

As demonstrated above, zero-dimensional (zero-D) modeling is typically conducted to validate chemical kinetic models against experimental RCM data while properly accounting for the heat loss and radical pool effects. Since the use of a creviced piston enables attainment of a nearly homogeneous temperature field inside the reaction chamber, using a creviced piston is expected to positively influence the validity of the zero-D modeling approach if the zero-D model is coupled with an adequate heat loss model. However, such a zero-D modeling approach based on an “adiabatic volume expansion” has to be critically assessed for the conditions of two-stage ignition. This is because significant heat release may occur during the first-stage ignition event as well as prior to the final hot-ignition event (i.e. during the second stage ignition). Consequently, the influence of multi-dimensional effects due to the presence of the boundary layer, cooler crevice zone, and non-uniform heat release could be significant. Although the use of a heat loss model in the zero-D modeling approach aims to capture the above-mentioned multi-dimensional effects, it is not clear *a priori* whether such an approach can be extended to the cases exhibiting two-stage ignition characteristics, even though it has been shown to be sufficient for single-stage ignition events [48].

A CFD modeling study of reactive *n*-heptane/oxidizer mixtures in an RCM with a creviced piston was undertaken to assess the validity of the zero-D modeling approach for ignition delay prediction under the conditions of two-stage ignition and NTC response [35]. *n*-Heptane was

taken as the candidate fuel because it is well known to exhibit strong NTC behavior and two-stage ignition phenomena. From the evolution of the temperature field during reaction, it was noted in [35] that at compressed temperatures close to the peak of the NTC response, reactions proceeded faster in the low-temperature region within the reaction chamber, which in turn smoothed out temperature inhomogeneity. Based on a comparison of the CFD simulations and zero-D calculations over the entire NTC regime, it was observed in [35] that the zero-D simulations predict the first-stage ignition delay times accurately but lead to a higher pressure rise in the first-stage ignition and consequently shorter total ignition delay times. However, the trend of the total ignition delay times is nicely reproduced by the zero-D approach [35]. In addition, the discrepancy in using the zero-D approach is pressure dependent and decreases as the compressed pressure increases. It also can be inferred from the comparison of computed pressure traces shown in [35] that the effective volume trace deduced from the non-reactive counterpart is still acceptable to be used in the corresponding zero-D modeling after the first-stage ignition event, at least for the conditions investigated. Although the creviced piston offers the advantage of suppression of the vortex, multi-dimensional effects are not completely avoided during the conditions of two-stage ignition. Nevertheless, when only single-stage ignition is present, the error introduced by zero-D simulations is considerably smaller [35].

Since CFD simulations of RCM experiments with detailed chemistry are not always a viable approach because of computational cost, the extent of agreement between the CFD and zero-D simulations could be improved by incorporating multiple zones, including the core region, boundary layer, and crevice, and allowing for the exchange of mass and energy between zones. Multi-Zone Modeling (MZM) has been applied to engine research for some time, see e.g. [60] and references therein. Several researchers have applied MZM to RCMs in order to improve model fidelity while retaining the simplicity and computational effort required for zero-D models [e.g., 29,61,62]. MZM typically divides the reaction chamber and piston assembly of the RCM into several zones, each of which are simulated separately. Zone interactions are handled by specifying energy- and mass-transfer boundary conditions. For example, recent work by Goldsborough *et al.* [61] divided the reaction chamber and piston into four zones, including the reaction chamber, the piston gap, the crevice volume, and the ringpack used to seal the piston in the reaction chamber. Using these zones, it was found [61] that the MZM results agreed very well with CFD results under non-reactive conditions, and the MZM results showed only slight differences from reactive CFD simulations. Furthermore, comparison of MZM and zero-D simulations with experimental data of  $H_2/O_2$  ignition showed similar agreement for both modeling methodologies, indicating the reliability of the new MZM method for predicting single-stage ignition events [61]. Two MZM-based methodologies to account for multi-stage ignition effects were recently proposed by Goldsborough *et al.* [62] in an attempt to improve the robustness of homogeneous reactor modeling of RCM experiments. It was shown [62] that increased heat losses from the reaction chamber are the primary source of extensions to ignition delay times during multi-stage ignition events. Although the improvements to predicted ignition delay times are reasonably good, some discrepancies were also noted [62]. Therefore, the authors indicated that additional work should be undertaken to address the discrepancies and to further validate the proposed methodology over a broader range of conditions.

Despite the potential of MZM and similar approaches to improve modeling fidelity relative to zero-D simulations, caution must still be exercised in using such approaches, since any complex model may introduce additional uncertainties due to the coupling of physical (i.e. heat loss and pressure drop) and chemical processes. Therefore, the benefits derived from introducing

a complex model may not be worth the cost, especially if the expected discrepancy from the zero-D approach is not excessive from the viewpoint of ignition delay prediction. It is further anticipated that the level of discrepancy will be fuel dependent. Thus, until these issues are better understood within the community, modelers should exercise caution in that zero-D simulated results may not predict well total ignition delay times under the conditions of two-stage ignition. Further investigation regarding the adequacy of zero-D RCM simulations for two-stage ignition response is warranted.

#### **4. Uncertainties and Issues for RCM Experiments**

Typically, in RCM experiments, ignition delay times are defined as the difference in time from the peak pressure measured at the end of compression to the rapid rise in pressure due to autoignition. Good design features to mitigate vibration at the end of compression will help minimize the uncertainties in setting a time zero (i.e. the end of compression) and the conditions at the end of compression. Subsequently, the onset of ignition can be defined, for instance, as the maximum rate of pressure rise in the post end-of-compression pressure record, both for the first stage ignition and the total (hot) ignition. A different definition of the ignition point, corresponding to 20% of the pressure rise due to ignition, was also used previously [63,64]. Each compressed pressure and temperature condition should be repeated several times to ensure repeatability and statistical significance. The mean and standard deviation of the ignition delay time for the repeated runs at each condition can then be calculated and reported.

The standard deviation of the experiments at a given condition is representative of the random error associated with RCM experiments. However, a detailed uncertainty propagation analysis is needed to determine the systematic uncertainty in the reported ignition delay times as functions of  $P_C$ ,  $T_C$ , and reactant composition. The systematic uncertainty in the measured ignition delay time arises from several sources, including the uncertainty in preparing the initial reactant mixture, the uncertainty in the measured pressure, and the uncertainty in the deduced compressed gas temperature. In the following, each potential source of errors will be briefly discussed and some best practices recommendations are given.

First, the uncertainty in the initial reactant concentrations is caused by several sources, including uncertainty in the partial pressure measurements of gaseous components and in the handling of liquid reactants. Furthermore, the extent of reactant adsorption/absorption on the metallic surface and the seals of the vacuum tank, reaction chamber, and feeding lines can be examined by individually filling the chamber with each test reactant studied and then monitoring the reaction chamber pressure as a function of time. If fuel/gas absorption occurs, the reaction chamber pressure will fall over time.

Although experimentation with gaseous fuels is relatively straightforward, the handling of liquid fuels may require heating of the RCM, and hence special care is needed to ensure the fuel is completely in the vapor phase. Given the target initial fuel partial pressure, the boiling point of the liquid fuel, and the volatility of the liquid fuel, the preheat temperature of the entire RCM can be determined such that the fuel will remain completely vaporized. Subsequently, it is important to ensure a uniform pre-heat temperature distribution within the reaction chamber, mixing tank, and feeding lines. Several approaches to vaporize the liquid fuel and prepare the initial premixed charge have been developed, including: (1) preparing the test homogeneous mixture in a separate heated mixing vessel of a known volume prior to being introduced to the reaction chamber [e.g., 65]; (2) feeding the reactants directly into the heated reaction chamber [e.g., 66]; and (3)

delivering the fuel to the reaction chamber in the form of an aerosol which, upon compression, forms a homogenous mixture [e.g., 67]. For any mixture preparation approach, a test protocol needs to be developed together with a detailed characterization to confirm the fuel vaporization and mixture homogeneity. In a recent high-pressure RCM study on the oxidation of *n*-propylbenzene ignition by Darcy *et al.* [68], fuel-air mixture compositions were verified by in situ testing using an infra-red laser system. The setup was similar to that developed by Mével *et al.* [69], who studied gas-phase absorption cross sections at 3.39  $\mu\text{m}$  to determine the concentration of twenty-one liquid hydrocarbons in the temperature range 303–413 K.

Further, the potential issues of mixture stratification and fuel condensation should be closely scrutinized. If the approach of preparing the test mixture in a separate vessel is followed, substantial heating time may be required to ensure the complete vaporization of the liquid component. In this approach, continuous stirring is needed to ensure a homogeneous mixture, for instance by using a magnetic stirrer [cf. 44,65,70–75]. In addition, the possibility of fuel cracking/pyrolysis within the mixture preparation vessel over an extended time period needs to be avoided, and characterization experiments should be conducted to confirm the assumptions of minimal/negligible fuel loss, mixture homogeneity, and non-decomposition of fuel in the mixture preparation vessel, as carried out in [e.g., 65,73,74].

In addition, the reaction chamber, mixing tank, and feeding lines must be kept clean. For instance, if the reaction chamber is cleaned with a solvent after a number of runs, some black deposits may be noted, especially if experiments have been run under fuel-rich conditions. One typical symptom of this condition is a peculiar pre-ignition pressure rise when the combustion chamber becomes contaminated after a number of successive runs, as demonstrated in [76] for the case of aromatic fuels. Also, the experimental results of two consecutive runs with the same condition were compared in [76], showing that once the reaction chamber is contaminated the experiment is no longer reproducible. However, when the reaction chamber is carefully purged and cleaned, ignition is highly reproducible. Note that it may also be possible to introduce surface effects into the reaction chamber if it is not cleaned carefully, for example, by removing any inert coating on the reaction chamber walls. It is noted that the shock tube experiments of Wang *et al.* [77] using  $\text{H}_2$ /air/steam mixtures also showed that the ignition process is very sensitive to the inner surface quality of the tube. Wang *et al.* [77] further demonstrated that if the tube is contaminated, their measured ignition delay time could not be reproduced. Thus, one must be sure that the experimental data acquired are free from the effect of chamber surface contamination.

Second, the uncertainty in the pressure measurements must be taken into account. There are two primary sources of uncertainty in the pressure measurement, including the uncertainty inherent in the transducer (usually specified by the manufacturer) and uncertainty related to the heat load applied to the transducer due to the rapid compression heating of the test gases. Further uncertainty may be introduced by the mounting procedure of the pressure transducer, including the mounting location and the torque applied to the threads during installation.

Since the effect of the head load on the transducer is generally difficult to detect, extra caution must be exercised. In particular, if the pressure transducer used in the study is not heat shock resistant, the rapid temperature increase of the gas in the reaction chamber during compression and the resulting heat loads to the transducer will change the output signal of the transducer, with the behavior depending on the thermal characteristics of the particular transducer assembly. To prevent this effect, the pressure transducer can be covered by a thin



silicone layer in the non-reactive experiments. This layer acts to shield the sensor against the heat load during the experiment. Thus, the temperatures at the end of compression in the reactive experiments are derived using the compression ratio determined in the corresponding non-reactive experiments. However, the reactive experiments have to be performed without the silicone layer since it can interfere with the chemical reactions under investigation, influencing the reactivity and leading to spurious ignition delay measurements. The heat shock can affect the rate of pressure rise, which may be reduced, but this is expected to have a negligible influence on the determination of the time of the ignition point and the end of compression. However, it should be noted that while assessment of ignition delay times can be reasonably accurate with an unprotected transducer, heat release rate analyses or the determination of first stage pressure/temperature rise cannot be conducted on experiments using the pressure transducers that do not have thermal protection.

Figure 13 shows the effect of the thermal protection layer using a pressure transducer (Kistler 603B) that is not thermal shock resistant [78]. The measured pressure in the comparative experiments is lower without the silicone thermal protection. Similar results were also shown in [38]. Since the temperature profile is deduced from the pressure profile then the temperature would also be lower than reality using the profiles from the non-shielded sensor. This would result in longer ignition delay times computed in the simulation compared to a simulation using the profile measured with the shielded sensor, as shown in Fig. 13. Therefore, the use of a thermal protection layer reduces uncertainties in the temperature of the experiment and the simulation. Similar observations have been reported in shock tube studies. RCM designers should thus consider using a pressure transducer that is not sensitive to thermal shock so that the problem of thermal shock can be eliminated for both non-reactive and reactive RCM experiments. Experiments by Mittal and Bhari [38] showed that when using a thermal-shock resistant pressure transducer, identical pressure traces were obtained with and without the use of a thermal protective coating. Furthermore, Mittal and Bhari [38] highlighted the importance of calibrating the dynamic pressure transducer used in the experiments.

Finally, the temperature at the end of compression is often taken as the reference temperature for reporting ignition delay data and can be obtained from Eq. (2). In general, the uncertainty in  $T_c$  is dependent on the uncertainties of the initial pressure and temperature, the compressed pressure, the initial mixture composition, and the fits for the specific heats of the mixture components. An error propagation analysis is needed to determine the contributions of these factors to the uncertainty of the calculation of the compressed temperature. Weber *et al.* [73] reported that the largest contributor to the total uncertainty in compressed temperature is the error in the initial pressure measurement, whereas the contributions from the measurements of the initial temperature and the compressed pressure are less significant. In addition, the uncertainty of  $T_c$  is dependent on the actual value of the initial pressure, but not on the values of the other quantities [73]. All other things being equal, higher initial pressures result in lower uncertainties in the compressed temperature. However, the study of Weber *et al.* [73] did not consider the influence of the uncertainty in the specific heat fits with respect to the compressed temperature. Instead, the uncertainty in the initial mixture composition, as measured by GCMS experiments, was used as the uncertainty in the specific heat ratio [73]. The overall uncertainty in the compressed temperature was not very sensitive to the uncertainty in the specific heat ratio; thus, the uncertainty in the specific heat fits should have only a small influence on the uncertainty of the compressed temperature. Taken all together, a conservative estimate of the total uncertainty in the compressed temperature of the core gases is about 0.7% to 1.7% [73].

Reducing this uncertainty can be accomplished most simply by improving the accuracy of the pressure transducer used to measure the initial pressure.

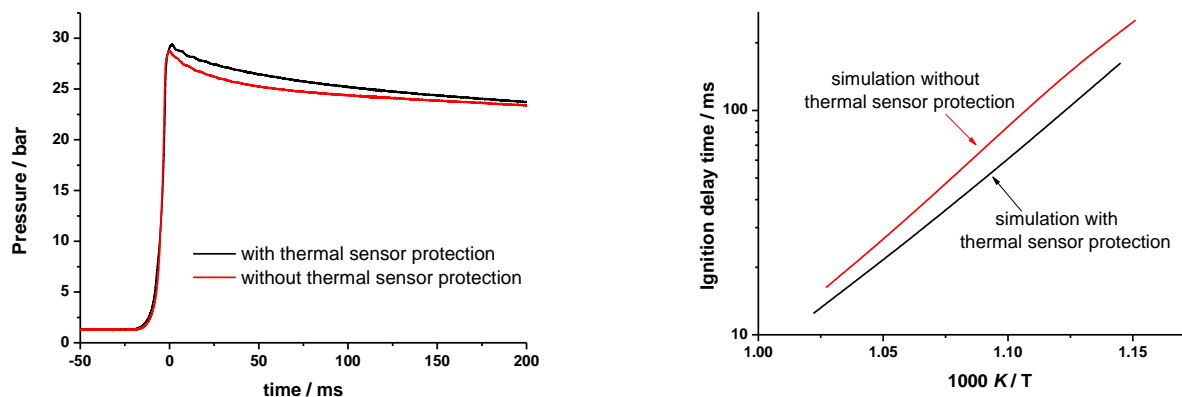


Fig. 13 – Results for 90% “natural gas” (81.25% CH<sub>4</sub>, 10% C<sub>2</sub>H<sub>6</sub>, 5% C<sub>3</sub>H<sub>8</sub>, 2.5% C<sub>4</sub>H<sub>10</sub>, and 1.25% C<sub>5</sub>H<sub>12</sub>) / 10% H<sub>2</sub>,  $\phi = 2.0$  in air. Left: Influence of thermal sensor protection on the pressure measurement in experiment. Right: Influence of different pressure profiles on simulation results [78].

## 5. Diagnostics in RCM Experiments

In an RCM experiment, the ignition event is marked by a rapid rise in the reaction chamber pressure measured directly using a pressure transducer. Apart from direct measurement of ignition delay time, ex-situ and in-situ speciation measurements can also be conducted to understand the evolution profile of different species. Direct visualization techniques such as Schlieren imaging and chemiluminescence have been used to examine the development of the combustion event [52,79,80]. Moreover, Guibert *et al.* [80] also performed an experimental investigation of the turbulence effect on combustion propagation using particle image velocimetry to determine flow characteristics prior to ignition in a rapid compression machine.

The determination of time-dependent species concentrations during the induction period provides the next level of rigor in model comparisons, extending the validation with global responses like ignition delay time. The capability of determining ignition delay times of various fuels and characterizing the temporal evolution of species concentration during ignition can help in the development of accurate chemical kinetic mechanisms for the fuels of interest.

Furthermore, direct measurement of the temperature-time history in an RCM experiment is highly desirable. If the RCM is designed with optical access to the reaction chamber in mind, the capability of non-intrusive direct measurements of the temperature- and species-time histories under a wide range of experimental conditions will widen the horizon of RCM research for combustion kinetics. Direct non-intrusive temperature measurement of the adiabatic core in the RCM is a challenge due to high pressure, noise, and machine vibration conditions. Nevertheless, there have been several previous efforts to directly measure the temperature inside RCMs using laser diagnostic techniques [e.g., 22,34,81–84].

Desgroux *et al.* [22] used a laser Rayleigh scattering technique to directly measure the core gas temperature in an RCM with 3–4 % measurement accuracy. However, the standard deviation of the measurements performed was around 10–15% near end of compression, which was

attributed to fluid motion and hence lack of homogeneity. It should be noted that a flat piston was used in [22]. Desgroux *et al.* [22] noted that background noise posed a major challenge in the temperature measurements. In a later study, Clarkson *et al.* [81] investigated the temperature field of reactive and non-reactive mixtures using acetone LIF and compared these to temperature fields imaged using Rayleigh scattering. They noted the relative insensitivity of the Rayleigh scattering method. Mittal and Sung [34] studied the temperature field of non-reactive mixtures using acetone PLIF. As noted earlier, the temperature field recorded by Mittal and Sung [34] for compression with a creviced piston was much more uniform compared to its flat piston counterpart. In a recent study, Strozzi *et al.* [82] used toluene PLIF to characterize an RCM temperature field for inert mixtures. However, in LIF studies, markers like toluene or acetone are not always present in combustible mixtures tested in RCMs; in addition, pyrolysis of these markers pose an additional complexity in the LIF measurements at higher temperatures.

The laser absorption technique adopted in [83,84] employed water line absorption in the mid-IR region using a quantum cascade laser to measure temperature-time histories. H<sub>2</sub>O absorption was used because of its universal presence in common combustion systems. Thus, this method can be further used for measurements in reactive mixtures where H<sub>2</sub>O is formed as a product of combustion. Water can also be present in amounts sufficient for detection even during the induction time. Water absorption lines near 7.6  $\mu\text{m}$  were used to determine the temperature history using the two-line ratio method, and both non-reactive and reactive mixtures with and without H<sub>2</sub>O doping have been studied [83,84]. The collisional broadening parameters of the water transition lines in the range of 1316.4–1317.8  $\text{cm}^{-1}$  with H<sub>2</sub>, O<sub>2</sub>, or Ar as a bath gas were also determined [83,84]. In order to isolate the effects of chemical reactions, an inert mixture of argon with 2.87% water vapor was used in [83]. The end of compression pressures and temperatures in the RCM measurements were  $P_C = 10, 15, \text{ and } 20$  bar in the temperature range of  $T_C = 1000\text{--}1200$  K. The measured temperature history was compared with that calculated based on the adiabatic core assumption and was found to be within  $\pm 5$  K. Furthermore, uncertainty analysis was conducted in [83] to examine the effect of the cold boundary layer by computing the predicted total absorbance, including the core and boundary layer, as a function of boundary layer thickness. Based on the computed total absorbance, the authors of [83] compared the deduced core temperature with the ideal core temperature (i.e. no boundary layer) and further compared the deduced number density of water to the actual doped number density (known). This analysis showed that the boundary layer thickness was less than 5% of the diameter of the reaction chamber and the mixture temperature was uniform across the reaction chamber [83,84]. In [84], temperature measurements in an RCM were successfully conducted for reactive mixtures of H<sub>2</sub>/O<sub>2</sub>/Ar at a compressed pressure of  $P_C \sim 11.5$  bar and a compressed temperature of  $T_C \sim 1022$  K, with and without water doping. A six-pass absorption setup was implemented in the RCM to detect very low concentrations of water. The temperatures obtained from simulations were within  $\pm 5$  K of the experimentally determined path-averaged temperatures for most of the cases when the simulated and experimental pressure traces were in agreement. Deviation of simulated temperatures from experimentally determined ones were noted for conditions when there is a notable difference in the pressure traces due to the discrepancy in the experimental and simulated ignition delay times. The reactive RCM experiments of [84] also indicated that the temperature-time history could be measured prior to ignition, even without doping, if the mixture produces sufficient water during the induction period.

Furthermore, the studies of [83,84] explored the possibility of measuring the time-dependent number density of water molecules, using the absolute absorption of two rovibrational lines. The

same studies also conducted an uncertainty analysis for temperature and water concentration measurements. For the conditions with no water doping, the uncertainties in temperature and water mole fraction measurements were 11% and 15.7%, respectively, for the worst case, while for the best condition they are 1.2% and 5.3%, respectively [84]. In general, the uncertainty in the measurement of water mole fraction for the case with water doping is within 5.2–6.1% [84]. It was further noted that the uncertainty analysis was carried out with a very conservative estimate for the uncertainty of the path length (5%) [84].

Other laser diagnostics used in RCM studies include measurements of soot volume concentration [85] and hydroxyl radical concentration [86,87]. In [85], the soot evolution was studied by the line-of-sight extinction method, which measured the soot concentration in the initial stage of soot growth before the optical path became opaque. Using OH laser absorption, the ignition and combustion kinetics of silane were investigated [86]. Furthermore, He *et al.* [87] measured OH concentrations using narrow line absorption centered at  $3206.556\text{ cm}^{-1}$  during *iso*-octane autoignition. The spectral line was chosen to minimize absorption from olefins and soot produced during the induction and ignition events, respectively. He *et al.* [87] estimated that the uncertainty associated with the OH measurements was approximately  $\pm 12\%$ . The measured OH profiles were further used to validate the rate constants of important reactions [87].

Ex-situ speciation measurements in RCMs are typically accomplished using a rapid sampling apparatus that enables extraction of the product mixture at specified post-compression times. The measured concentrations of intermediate species in an RCM experiment provide additional model constraining data beyond the global ignition delay times. In order to freeze the reaction at the desired instance, fast quenching of the reacting mixture is required. Early work in species sampling from RCMs was performed by quenching the entire reaction chamber [e.g., 16,19,88–91], including the boundary layer in the reaction chamber and the piston crevice volume. Depending on the piston head designs, the crevice volume may be as much as, or more than, 20% of the final reaction chamber volume. This may lead to increased uncertainty in the species mole fractions as un-reacted fuel and oxidizer from the crevice volume are incompletely mixed with the core gas during sampling and quenching. More recent work has focused on using fast sampling valves inserted into the core volume to remove small quantities of gas for analysis without significantly disrupting the ongoing chemical reactions. The valve is inserted through the end- or side-wall of the reaction chamber so that it protrudes into the adiabatic core volume and is triggered at defined times during the induction period to withdraw samples, which are typically sent to GC/FID or GC/TCD for analysis. By performing several experimental runs sequentially and slightly changing the valve trigger delay, time-resolved species profiles may be measured throughout the entire ignition induction period. The fast sampling valve technique is still relatively new, and the uncertainty associated with such measurements has not been considered in depth. It is expected that the sampling probe will have a minimal effect on the flow field, due to its small size, but this has not been confirmed either experimentally or computationally. Furthermore, it is unclear how the boundary layer surrounding the probe surface might affect the speciation results.

Recent work has focused on primary reference fuels (PRFs), biofuels, and biofuel/PRF blends, including work with *n*-heptane [92], *iso*-octane [93], *n*-butanol [94], *n*-heptane/*n*-butanol blends [95], and methyl-butanoate [96]. These studies found that, although most chemical kinetic models are able to predict the ignition delay time fairly well (e.g., within 20% typically), the predictions of some species profiles deviate from those measured experimentally, and this may

influence the model's ability to predict combustion features besides ignition delay time, e.g., soot formation and/or emissions. Subsequently, the results from these experiments were used to direct improvements of the species profile predictions by updating rate constants with newly measured or calculated rates from the literature. Despite the work to date, there is very little quantitative speciation data available in the literature from RCMs and more studies are required to flesh out the reaction pathways of common fuels under engine relevant conditions, especially new biofuels. Significant opportunities therefore exist for RCM measurements towards further improving our understanding of combustion chemistry, especially measurements that are difficult to perform in shock tubes and other devices, including within the NTC regime, as well as quantification of features associated with early heat release. For instance, the advanced absorption spectroscopy techniques developed at Stanford University [1] to measure concentrations of  $\text{CH}_3$  and  $\text{OH}$  radicals and  $\text{CO}_2$ ,  $\text{H}_2\text{O}$ ,  $\text{C}_2\text{H}_4$ , and fuel as a function of time in a shock tube could also be applied in RCM studies. Moreover, Ihme *et al.* [97] recently performed detailed simulations of shock-bifurcation and ignition of an argon-diluted hydrogen/oxygen mixture in a shock tube and highlighted complex physics that can occur in shock tubes that is not well understood. This complexity can limit performance in shock tubes. This gives motivation and benefit of utilizing RCMs to access various thermodynamic regimes. To this end, Ihme [98] simulated the autoignition of syngas mixtures in an RCM by considering the interaction between turbulence, detailed reaction chemistry, and wall heat-loss effects. Turbulence-generation during the filling process, corner vortices, wall-generated turbulence, and mixing between the fluid in the core region and in the boundary layer were all found to contribute to the generation of inhomogeneities in flow-field, temperature, and mixture composition. A Damköhler criterion was proposed in order to characterize the sensitivity of the induction chemistry to turbulence fluctuations. It was found that syngas mixtures with Damköhler numbers below 50 exhibited increasing sensitivity to turbulence and mixture fluctuations. The study of Ihme [98] indicated that the turbulence-chemistry interaction can be equally as important as chemical kinetic and hydrodynamic processes in affecting syngas ignition timing and requires consideration.

## 6. Concluding Remarks and Future Directions

This paper reviews the experimental and computational efforts applying RCMs to chemical kinetic studies. Much effort has been expended to demonstrate that the RCM is a reliable facility to use in these studies, provided care is taken in designing the facility and in interpreting the experimental results. Recent progress in RCM research, including novel design improvements and experimental approaches as well as advanced ex-situ and in-situ diagnostics and computational methods, can provide useful insights into fundamental autoignition chemistry in thermodynamic regimes that are difficult to access in other experimental apparatuses.

The ability for fast compression and vibration-free piston stopping without bounce are the prime requirements of an RCM. Moreover, the existence of a thermodynamically well-defined core region of compressed gas mixture is essential. Additional features such as optical accessibility for in-situ non-intrusive laser/optical diagnostics, the ability to vary stroke and clearance to achieve variable compression ratios, and the ability to rapidly extract the reacting mixture for species analysis are important to carry out various diagnostic studies under a wide range of experimental conditions.

Further design effort to expand the RCM operation envelope to encompass a wide range of conditions relevant to conventional and advanced internal combustion engines is encouraged.

RCM experiments with nonvolatile liquid fuels, such as bio-diesels, remain a challenge and require careful consideration for preparation of homogenous mixtures over extensive experimental conditions without fuel condensation and cracking.

In modeling RCM experiments one needs to simulate both the compression phase, to include any reaction during compression, and the post end-of-compression constant volume phase, to account for heat losses. Therefore, in addition to ignition delay times, experimental pressure traces for reactive runs and the corresponding non-reactive runs should be provided by experimenters so that the heat loss characteristics and hence volume history can be deduced from the non-reactive pressure traces for the subsequent reactive modeling. In addition, the adequacy of zero-dimensional modeling for simulating two-stage ignition phenomena merits further assessment.

Furthermore, validation of chemical kinetic models using ignition delay data gathered in shock tubes and rapid compression machines under low-to-intermediate temperature conditions strongly depends on the proper interpretation of experimental data [49]. Examples have been presented which show that ignition delay times measured under these conditions cannot be directly compared between different RCM and/or shock tube studies without accounting for “facility dependent” effects. Therefore, for RCM modeling in particular, it is important to simulate the entire processes occurring in the experiment, including the compression stroke.

Developing an advanced methodology for direct temperature measurements in RCMs is highly desirable. Path-averaged temperatures measured using the two-line absorption method have been shown to be in very good agreement with calculated temperature histories using zero-D modeling based on the adiabatic core assumption [83,84]. When the effect of vortex roll-up is suppressed, the adiabatic core assumption for calculating the temperature evolution inside an RCM proves adequate for inert experiments as well as for the reactive experiments prior to the occurrence of appreciable heat release. In the presence of heat release (e.g., after the first stage of two-stage ignition) the adiabatic core hypothesis has not been fully validated for temperature estimation. The non-intrusive direct temperature determination method should be extended to obtain the temperature history of reactive systems inside the RCM, as well as assess the effect of cold edges.

Finally, the development of ex-situ and in-situ methods for facilitating speciation measurements is also of significance. Several studies have been conducted to validate the ability of chemical kinetic models to predict the species profiles during the ignition delay period. However, due to the novelty of such techniques, only a few conditions have been considered. The availability of in-situ multi-species time history measurements in RCMs, especially for pressures up to 50–100 bar, would be a valuable tool for the understanding of low-to-intermediate temperature chemistry.

## **Acknowledgments**

Preparation of this review was supported by the Combustion Energy Frontier Research Center, an Energy Frontier Research Center funded by the US Department of Energy, Office of Basic Energy Sciences under Award Number DE-SC0001198. We would like to thank Prof. John Simmie, Dr. Judith Würmel, Dr. Alexander Heufer, Dr. Rory Monaghan, Dr. Nicola Donohoe, Mr. Robert Richardson, Mr. Bryan Weber, and Mr. Goutham Kukkadapu for helpful discussions and some figures in preparing this manuscript. CJS also wishes to acknowledge the financial support received from National Science Foundation, Department of Energy, Army Research Office, National Aeronautics and Space Administration, and Air Force Office of Scientific Research as well as from industry in supporting rapid compression machine research over the years.

## References

- [1] Hanson RK, Davidson DF. The role of laser absorption techniques and modern shock tube methods in studies of combustion chemistry. Under review.
- [2] Argonne National Laboratory [Internet]. Chicago: U.S. Department of Energy Office of Science; c2000-13 [updated 2013 Jan; cited 2014 Mar]. 1<sup>st</sup> International RCM Workshop. Available from:  
[http://www.transportation.anl.gov/rcmworkshop/1st\\_workshop/index.html](http://www.transportation.anl.gov/rcmworkshop/1st_workshop/index.html).
- [3] Falk KG. The ignition temperatures of hydrogen-oxygen mixtures. J Amer Chem Soc. 1906; 28:1517-34.
- [4] Dixon HB, Bradshaw L, Campbell C. The firing of gases by adiabatic compression. Part I. photographic analysis of the flame. J Chem Soc Trans. 1914;105:2027-35.
- [5] Dixon HB, Crofts JM. The firing of gases by adiabatic compression. Part II. the ignition-points of mixtures containing electrolytic gas. J Chem Soc Trans. 1914;105:2036-53.
- [6] Cassel H. Über Entflammung und Verbrennung von Sauerstoff-Wasserstoff-Gemischen. Annalen der Physik. 1917;356:685-704.
- [7] Tizard HT. The cause of detonation in internal combustion engines. North-East Coast Institution of Engineers and Shipbuilders, 1920-1.
- [8] Tizard HT, Pye DR. Experiments on the ignition of gases by sudden compression. Philosophical Magazine 1922;44:79-121.
- [9] Tizard HT, Pye DR. Ignition of gases by sudden compression. Philosophical Magazine 1926;1:1094-105.
- [10] Aubert M. Étude Physico-Chimique de Quatre Combustible Liquides Extraits d'un Goudron Primaire, Obtenue à Partir des Déchets d'Extraction des Mines Domaniales Françaises de la Sarre. Chaleur et Industrie'. 1929;6:373-9.
- [11] Fenning RW, Cotton FT. Experiments on the ignition of gases by sudden compression. Reports and memoranda, Great Britain Aeronautical Research Committee, 1930.
- [12] Affleck WS, Thomas A. An opposed piston rapid compression machine for pre-flame reaction studies. Proc Inst Mech Eng. 1968;183:365-87.
- [13] Carlier M, Corre C, Minetti R, Pauwels J-F, Ribaucour M., Sochet L-R. Autoignition of butane: a burner and a rapid compression machine study. Proc Combust Inst. 1991;23:1753-8.
- [14] Griffiths JF, Jiao Q, Schreiber M, Meyer J, Knoche KF. Development of Thermokinetic Models for Autoignition in a CFD Code: Experimental Validation and Application of the Results to Rapid Compression Studies. Proc Combust Inst. 1992;24:1809-15.
- [15] Park P. Ph.D. 1990 Massachusetts Institute of Technology  
<http://hdl.handle.net/1721.1/14068>.
- [16] Mittal G, Sung CJ. A rapid compression machine for chemical kinetics studies at elevated pressures and temperatures. Combust Sci Tech. 2007;179(3):497-530.



- [17] Donovan MT, He X, Palmer TR, Zigler BT, Wooldridge MS, Atreya A. Demonstration of a free-piston rapid compression facility for the study of high temperature combustion phenomenon. *Combust Flame*. 2004;137:351-65.
- [18] Rogowski AR. A new machine for studying combustion of fuel sprays with controlled air motion. SAE Preprint. 1963;436F.
- [19] Minetti R, Ribaucour M, Carlier M, Fittschen C, Sochet LR. Experimental and modeling study of oxidation and autoignition of butane at high pressure. *Combust Flame*. 1994;96:201-11.
- [20] Hu H, Keck J. Autoignition of adiabatically compressed combustible gas mixtures. SAE Tech. Paper 872110, 1987.
- [21] Griffiths JF, Jiao Q, Schreiber A, Meyer J, Knoche KF, Kardylewski W. Experimental and numerical studies of ditertiary butyl peroxide combustion at high pressure in a rapid compression machine. *Combust Flame*. 1993;93:303-15.
- [22] Desgroux P, Gasnot L, Sochet LR. Instantaneous temperature measurement in a rapid-compression machine using laser rayleigh scattering. *Applied Physics B*. 1995;61:69-72.
- [23] Minetti R, Carlier M, Ribaucour M, Therssen E, Sochet LR. Comparison of oxidation and autoignition of the two primary reference fuels by rapid compression. *Proc Combust Inst*. 1996;26:747-53.
- [24] Griffiths JF, Halford-Maw PA, Mohamed C. Spontaneous ignition delays as a diagnostic of the propensity of alkanes to cause engine knock. *Combust Flame*. 1997;111:327-37.
- [25] Silke EJ, Curran HJ, Simmie JM. The influence of fuel structure on combustion as demonstrated by the isomers of heptane: a rapid compression machine study. *Proc Combust Inst*. 2005;30:2639-47.
- [26] Würmel J, Simmie JM. CFD studies of a twin-piston rapid compression machine. *Combust Flame*. 2005;141:417-30.
- [27] Würmel J. Detailed chemical kinetics combined with a computational fluid dynamics study of a twin piston rapid compression machine [PhD Thesis]. Galway: National University of Ireland; 2004.
- [28] Daneshyar H, Fuller DE, Deckker BEL. Vortex motion induced by the piston of an internal combustion engine. *Int J Mech Sci*. 1973;15:381-90.
- [29] Lee D, Hochgreb S. Rapid compression machine: heat transfer and suppression of corner vortex. *Combust Flame*. 1998;114:531-45.
- [30] Clarkson J, Griffiths JF, MacNamara JP, Whitaker BJ. Temperature fields during the development of combustion in a rapid compression machine. *Combust Flame*. 2001;125:1162-75.
- [31] Griffiths JF, Macnamara JP, Mohamed C, Whitaker BJ, Pan J, Sheppard CGW. Temperature fields during the development of autoignition in a rapid compression machine. *Faraday Discuss*. 2002;119:287-303.

- [32] Griffiths JF, MacNamara JP, Sheppard CGW, Turton DA, Whitaker BJ. The relationship of knock during controlled autoignition to temperature inhomogeneities and fuel reactivity. *Fuel*. 2002;81:2219-25.
- [33] Desgroux P, Minetti R, Sochet LR. Temperature distribution induced by pre-ignition reactions in a rapid compression machine. *Combust Sci. Tech*. 1996;113:193-203.
- [34] Mittal G, Sung CJ. Aerodynamics inside a rapid compression machine. *Combust Flame*. 2006;145:160-80.
- [35] Mittal G, Raju MP, Sung CJ. CFD modeling of two-stage ignition in a rapid compression machine: assessment of zero-dimensional approach. *Combust Flame*. 2010;157(7):1316-24.
- [36] Mittal G, Raju MP, Bhari A. A numerical assessment of the novel concept of crevice containment in a rapid compression machine. *Combust Flame*. 2011;158(12):2420-7.
- [37] Mittal G, Gupta S. Computational assessment of an approach for implementing crevice containment in rapid compression machines. *Fuel*. 2012;102:536-44.
- [38] Mittal G, Bhari A. A rapid compression machine with crevice containment. *Combust Flame*. 2013;160(12):2975-81.
- [39] Mittal G, Chomier M. Effect of crevice mass transfer in a rapid compression machine. *Combust Flame*. 2014;161(2):398-404.
- [40] Mittal G, Raju MP, Sung CJ. Vortex formation in a rapid compression machine: influence of physical and operating parameters. *Fuel*. 2012;94:409-17.
- [41] Ribaucour M, Minetti R, Sochet LR, Curran HJ, Pitz WJ, Westbrook CK. Ignition of isomers of pentane: an experimental and kinetic modeling study. *Proc Combust Inst*. 2000;28:1671-8.
- [42] Westbrook CK, Pitz WJ, Boercker JE, Curran HJ, Griffiths JF, Mohamed C, Ribaucour M. Detailed chemical kinetic reaction mechanisms for autoignition of isomers of heptane under rapid compression. *Proc Combust Inst*. 2002;29:1311-8.
- [43] Tanaka S, Ayala F, Keck JC. A reduced chemical kinetic model for HCCI combustion of primary reference fuels in a rapid compression machine. *Combust Flame*. 2003;133:467-81.
- [44] Weber BW, Sung CJ. Comparative autoignition trends in the butanol isomers at elevated pressure. *Energy and Fuels*. 2013;27(3):1688-98.
- [45] Sarathy SM, Park S, Weber BW, Wang W, Veloo PS, Davis AC, Togbé C, Westbrook CK, Park O, Dayma G, Luo Z, Oehlschlaeger MA, Egolfopoulos FN, Lu T, Pitz WJ, Sung C-J, Dagaut P. A comprehensive experimental and modeling study of iso-pentanol combustion. *Combust Flame*. 2013;160(12):2712-28.
- [46] Mittal G, Chaos M, Sung CJ, Dryer FL. Dimethyl ether autoignition in a rapid compression machine: experiments and chemical kinetic modeling. *Fuel Processing Technology*. 2008;89(12):1244-54.

- [47] Mittal G, Sung CJ, Fairweather M, Tomlin AS, Griffiths JF, Hughes KJ. Significance of the  $\text{HO}_2 + \text{CO}$  reaction during the combustion of  $\text{CO} + \text{H}_2$  mixtures at high pressures. *Proc Combust Inst.* 2007;31:419-27.
- [48] Mittal G, Raju MP, Sung CJ. Computational fluid dynamics modeling of hydrogen ignition in a rapid compression machine. *Combust Flame.* 2008;155:417-28.
- [49] Dryer FL, Chaos M. Ignition of syngas/air and hydrogen/air mixtures at low temperatures and high pressures: experimental data interpretation and kinetic modeling implications. *Combust Flame.* 2008;152:293-9.
- [50] Chaos M, Dryer FL. Syngas combustion kinetics and applications. *Combust Sci Tech.* 2008;180:1051-94.
- [51] He X, Donovan MT, Zigler BT, Palmer TR, Walton SM, Wooldridge MS, Atreya A. An experimental and modeling study of iso-octane ignition delay times under homogeneous charge compression ignition conditions. *Combust Flame.* 2005;142:266-75.
- [52] Walton SM, He X, Zigler BT, Wooldridge MS. An experimental investigation of the ignition properties of hydrogen and carbon monoxide mixtures for syngas turbine applications. *Proc Combust Inst.* 2007;31:3147-54.
- [53] Healy D, Kalitan DM, Aul CJ, Petersen EL, Bourque G, Curran HJ. Oxidation of C1–C5 alkane quaternary natural gas mixtures at high pressures. *Energy Fuels* 2010;24(3):1521-8.
- [54] Gallagher SM, Curran HJ, Metcalfe WK, Healy D, Simmie JM, Bourque G. A rapid compression machine study of the oxidation of propane in the negative temperature coefficient regime. *Combust Flame.* 2008;153:316-33.
- [55] Herzler J, Jerig L, Roth P. Shock tube study of the ignition of propane at intermediate temperatures and high pressures. *Combust Sci Technol.* 2004;176:1627-37.
- [56] Petersen EL, Lamnaouer M, de Vries J, Curran H, Simmie J, Fikri M, Schulz C, Bourque G. Discrepancies between shock tube and rapid compression machine ignition at low temperatures and high pressures. *Shock Waves.* 2009;1:739-44.
- [57] Davidson DF, Hanson RK. Recent advances in shock tube/laser diagnostic methods for improved chemical kinetics measurements. *Shock Waves.* 2009;19:271-83.
- [58] Pang GA, Davidson DF, Hanson RK. Experimental study and modeling of shock tube ignition delay times for hydrogen-oxygen-argon mixtures at low temperatures. *Proc Combust Inst.* 2009;32:181-8.
- [59] Chaos M, Dryer FL. Chemical-kinetic modeling of ignition delay: considerations in interpreting shock tube data. *Int J Chem Kinet.* 2010;42:143-50.
- [60] Kodavasal J, Keum S, Babajimopoulos A. An extended multi-zone combustion model for PCI simulation. *Combust Theory Mod.* 2011 Dec;15(6):893-910.
- [61] Goldsborough SS, Banyon C, Mittal G. A computationally efficient, physics-based model for simulating heat loss during compression and the delay period in RCM experiments. *Combust Flame.* 2012 Dec;159(12):3476-92.

- [62] Goldsborough SS, Mittal G, Banyon C. Methodology to account for multi-stage ignition phenomena during simulations of RCM experiments. *Proc Combust Inst.* 2013;34(1):685-93.
- [63] Tanaka S, Ayala F, Keck JC, Heywood JB. Two-stage ignition in HCCI combustion and HCCI control by fuels and additives. *Combust Flame.* 2003;132:219-39.
- [64] Di Sante R. Measurements of the auto-ignition of *n*-heptane/toluene mixtures using a rapid compression machine. *Combust Flame.* 2012;159:55-63.
- [65] Kumar K, Mittal G, Sung CJ. Autoignition of *n*-decane under elevated pressure and low-to-intermediate temperature conditions. *Combust Flame.* 2009;156:1278-88.
- [66] Allen C, Toulson E, Edwards T, Lee T. Application of a novel charge preparation approach to testing the autoignition characteristics of JP-8 and camelina hydroprocessed renewable jet fuel in a rapid compression machine. *Combust Flame.* 2012;159(9):2780-8.
- [67] Allen C, Mittal G, Sung CJ, Toulson E, Lee T. An aerosol rapid compression machine for studying energetic-nanoparticle-enhanced combustion of liquid fuels. *Proc Combust Inst.* 2011;33(2):3367-74.
- [68] Darcy D, Nakamura, H, Tobin, CJ, Mehl M, Metcalfe WK, Pitz, WJ, Westbrook CK, Curran HJ. A high-pressure rapid compression machine study of *n*-propylbenzene ignition. *Combust Flame.* 2014;161(1):65-74.
- [69] Mével R, Boettcher PA, Shepherd JE. Absorption cross section at 3.39 mm of alkanes, aromatics and substituted hydrocarbons. *Chem Phys Lett.* 2012;531:22-7.
- [70] Kumar K, Sung CJ. An experimental study of the autoignition characteristics of conventional jet fuel/oxidizer mixtures: Jet-A and JP-8. *Combust Flame.* 2010;157(4):676-85.
- [71] Kumar K, Sung CJ. A comparative experimental study of the autoignition characteristics of alternative and conventional jet fuel/oxidizer mixtures. *Fuel.* 2010;89(10):2853-63.
- [72] Kumar K, Sung CJ. Autoignition of methanol: experiments and computations. *International Journal of Chemical Kinetics.* 2011;43(4):175-84.
- [73] Weber BW, Kumar K, Zhang Y, Sung CJ. Autoignition of *n*-butanol at elevated pressure and low to intermediate temperature. *Combust Flame.* 2011;158(5):809-819.
- [74] Das AK, Sung CJ, Zhang Y, Mittal G. Ignition delay study of moist hydrogen/oxidizer mixtures using a rapid compression machine. *International Journal of Hydrogen Energy.* 2012;37(8):6901-11.
- [75] Kukkadapu G, Kumar K, Sung CJ, Mehl M, Pitz WJ. Experimental and surrogate modeling study of gasoline ignition in a rapid compression machine. *Combust Flame.* 2012;159(10): 3066-78.
- [76] Mittal G, Sung CJ. Autoignition of toluene and benzene at elevated pressures in a rapid compression machine. *Combust Flame.* 2007;150:355-68.
- [77] Wang BL, Olivier H, Grönig H. Ignition of shock-heated H<sub>2</sub>-air-steam mixtures. *Combust Flame.* 2003;133:93-106.
- [78] Heufer KA, Donohoe N, Curran HJ. Private Communication, 2014.

- [79] Strozzi C, Mura A, Sotton J, Bellenoue M. Experimental analysis of propagation regimes during the autoignition of a fully premixed methane-air mixture in the presence of temperature inhomogeneities. *Combust Flame*. 2012;159:3323-41.
- [80] Guibert P, Kéromnès A, Legros G. An experimental investigation of the turbulence effect on the combustion propagation in a rapid compression machine. *Flow Turbul Combust*. 2010;84(1):79-95.
- [81] Clarkson J, Griffiths JF, Macnamara JP, Whitaker BJ. Temperature fields during the development of combustion in a rapid compression machine. *Combust Flame*. 2001;125(3):1162-75.
- [82] Strozzi C, Sotton J, Mura A, Bellenoue M. Characterization of a two dimensional temperature field within a rapid compression machine using a toluene planar laser induced fluorescence imaging technique. *Meas Sci Technol*. 2009;20:125403.
- [83] Uddi M, Das AK, Sung CJ. Temperature measurements in a rapid compression machine using Mid-IR H<sub>2</sub>O absorption spectroscopy near 7.6  $\mu$ m. *Applied Optics*. 2012;51(22):5464-76.
- [84] Das AK, Uddi M, Sung CJ. Two-line thermometry and H<sub>2</sub>O measurement for reactive mixtures in rapid compression machine near 7.6  $\mu$ m. *Combust Flame*. 2012;159(12):3493-501.
- [85] Kitsopanidis I, Cheng WK. Soot formation study in a rapid compression machine. *Journal of Engineering for Gas Turbines and Power*. 2006;128(4):942-9.
- [86] Donovan MT, He X, Zigler BT, Palmer TR, Walton SM, Wooldridge MS. Experimental investigation of silane combustion and particle nucleation using a rapid compression facility. *Combust Flame*. 2005;141:360-70.
- [87] He X, Zigler BT, Walton SM, Wooldridge MS, Atreya A. A rapid compression facility study of OH time histories during iso-octane ignition. *Combust Flame*. 2006;145:552-70.
- [88] Roblee LHS. Technique for sampling reaction intermediates in a rapid compression machine. *Combust Flame*. 1961;5:229-34.
- [89] Beeley P, Griffiths JF, Gray P. Rapid compression studies on spontaneous ignition of isopropyl nitrate, part II: rapid sampling, intermediate stages and reaction mechanisms. *Combust Flame*. 1980;39:269-81.
- [90] Minetti R, Ribaucour M, Carlier M, Therssen E, Sochet LR. A rapid compression machine investigation of oxidation and auto-ignition of n-heptane: measurements and modeling. *Combust Flame*. 1995;102:298-309.
- [91] Cox A, Griffiths JF, Mohamed C, Curran HJ, Pitz WJ, Westbrook CK. Extents of alkane combustion during rapid compression leading to single-and two-stage ignition. *Symposium (International) on Combustion*. 1996 Jan;26(2):2685-92.
- [92] Karwat DMA, Wagnon SW, Wooldridge MS, Westbrook CK. Low-temperature speciation and chemical kinetic studies of n-heptane. *Combust Flame*. 2013; 160(12):2693-2706.

- [93] He X, Walton SM, Zigler BT, Wooldridge MS, Atreya A. An experimental investigation of the intermediates of iso-octane during ignition. *International Journal of Chemical Kinetics*. 2007;39:498-517.
- [94] Karwat DMA, Wagnon SW, Teini PD, Wooldridge MS. On the chemical kinetics of n-butanol: ignition and speciation studies. *The Journal of Physical Chemistry A*. 2011 May;115(19):4909-21.
- [95] Karwat DMA, Wagnon SW, Wooldridge MS, Westbrook CK. On the combustion chemistry of n-heptane and n-butanol blends. *The journal of physical chemistry A*. 2012 Dec;116(51):12406-21.
- [96] Walton SM, Karwat DMA, Teini PD, Gorny AM, Wooldridge MS. Speciation studies of methyl butanoate ignition. *Fuel*. 2011 May;90(5):1796-804.
- [97] Ihme M, Sun Y, Deterding R. Detailed simulations of shock-bifurcation and ignition of an argon-diluted hydrogen/oxygen mixture in a shock tube. *AIAA* 2013-0538.
- [98] Ihme M. On the role of turbulence and compositional fluctuations in rapid compression machines: Autoignition of syngas mixtures. *Combust Flame*. 2012;159(4):1592-604.